

## Resume

**Name:** Surajit Dhara  
**Date of Birth:** November 1<sup>st</sup>, 1970  
**Sex:** Male  
**Country of origin:** India  
**Country of current location:** India (relocated in April 2010)  
**Address:**

<p><i>Office:</i> National Institute of Biomedical Genomics (NIBMG), Kalyani, WB, India. PIN: 741251 Telephone: +91-33-25892151-Ext-253 Fax: +91-33-25892150 E-mail: <a href="mailto:sd1@nibmg.ac.in">sd1@nibmg.ac.in</a> <a href="mailto:surajit_dhara@hotmail.com">surajit_dhara@hotmail.com</a> Website: <a href="http://www.nibmg.ac.in">http://www.nibmg.ac.in</a></p>	<p><i>Residential:</i> Block-1, Flat-1C, Orbit Sky View 1/1A Umakanto Sen Lane, Pike Para, Kolkata, 700030 Cell phone: 9163280474</p>
---	---

### **Education:**

- **Ph.D.**, Physiology, All India Institute of Medical Sciences (AIIMS), 2002
- **M.Sc.**, Physiology with Biochemistry specialization, Calcutta University, 1993
- **B.Sc.**, Physiology, Calcutta University, 1991

### **Current Position:**

Scientist, April 2010 till date: National Institute of Biomedical Genomics (NIBMG), Kalyani, India.

### **Past Appointments:**

- Research Associate (Faculty), January 2010 to March 2010: Russell H. Morgan Department of Radiology and Radiological Sciences, The Johns Hopkins University School of Medicine, Baltimore, Maryland, U.S.A.
- Postdoctoral fellow, April 2003 to 2009, The Johns Hopkins University School of Medicine, Baltimore, MD, USA
- Postdoctoral fellow, August 2002 to April 2003, University of Minnesota, Minneapolis, MN, USA.
- Senior Demonstrator, September 2000 to August 2002. All India Institute of Medical Sciences (AIIMS), New Delhi, India.
- Research fellow and graduate student, April 1995 to August 2000, All India Institute of Medical Sciences (AIIMS), New Delhi, India.
- Research fellow, April 1994 to March 1995, Calcutta University, Kolkata, India.

### **Area of expertise:**

I have 14 years of research experience in the field of Cancer Experimental Therapeutics. I am an expert in the designing of novel cell-based assay systems and analytically frameworks which, along with the state of the art high throughput genomic/transcriptomic technologies, could be

utilized as unique discovery tools in cancer. Currently am heading a small research laboratory investigating cellular and molecular basis of chemotherapy response in glioblastoma multiforme and head & neck cancers.

**Ongoing projects in my laboratory:**

1. ***Improving temozolomide (TMZ) chemotherapy response in glioblastoma multiforme (GBM):*** In spite of dismal prognosis a small subgroup of GBM patients survives for significantly longer time than the others. We have recently discovered that the hedgehog (Hh) signaling pathway remains significantly suppressed in these patient-derived neoplastic cells possibly favoring their response to temozolomide (TMZ) treatment. We are currently exploring the possibility of improving TMZ response in this malignancy by experimentally suppressing this pathway utilizing our uniquely designed laboratory model systems.
2. ***Understanding genetic basis of chemoresistance in gingivobuccal squamous cell carcinoma (GBSCC):*** Though surgery is the mainstay of intervention in GBSCC majority of these cancers present late and therefore multimodality treatment is required. As a standard protocol an aggressive taxol-cisplatin-5-FU (TPF)-based chemotherapy comes into an algorithm of 1/3 of patients who present with advanced diseases. Our goal is to identify predictive biomarkers for TPF-chemotherapy response in this malignancy.

**Academic achievements thus far:**

- A. **Pioneered the concept** of involvement of the Hh-pathway in cancer metastasis, while doing my postdoctoral training at the Johns Hopkins University.
- B. **With a novel method we recently discovered** sonic hedgehog (Hh) pathway to hinder temozolomide (TMZ) chemotherapy response in glioblastoma multiforme. Inhibition of Hh-pathway could be a potential strategy to improve sustained TMZ-response in this malignancy.
- C. ***Setting up a functional laboratory:*** I have built a state of the art laboratory in my new institute. Here I have developed the pipeline for establishing GBM patient-derived neurospheres in collaboration with local hospitals. Also, developed a progressive cohort (N=90) CNS malignancies with clinical data, follow-up information, samples of blood and tumor tissues.
- D. ***Extramural grant:*** I have received a grant award from the Department of Biotechnology (DBT), Govt. of India.
- E. ***Building collaborations:*** In last few years, I have built up active collaborations with clinicians and scientists at the University of Pittsburgh, PA, USA, Memorial Sloan Kettering Cancer Center, NY, USA, Tata Memorial Hospital, Mumbai, India, AMRI Hospitals, Kolkata, India, Medica Superspeciality Hospital, Kolkata, India, Bangur Institute of Neurology, Kolkata, India, IPGMER, Kolkata, India and NRS hospital, Kolkata, India. We wrote research projects and also recently started to publish research papers together.

F. **Teaching:** In addition to direct mentoring as supervisor, I teach “Cancer Biology” for NIBMG Ph. D. program. I also served as a Senior Demonstrator in AIIMS teaching medical graduate and nursing students for two years, from 2000 to 2002.

G. **Administrative services:** I have been actively serving as the convener of NIBMG Ethical Committee, RCPRRH (Review Committee for the Protection of Research Risk in Humans) from 2010 till date.

**Fellowships & Memberships of Professional Societies:**

- Associate member of AACR (American Association for Cancer Research)
- Life member of the ISSRF (Indian Society for the Study of Reproduction and Fertility)
- Life member of the APPI (Association of Physiologists and Pharmacologists of India)

**Orations & Special Lectures:**

- Sydney Kimmel Cancer Center, Johns Hopkins University School of Medicine, Baltimore, USA. May 2007
- Russell Morgan Department of Radiology and Radiological Sciences, Johns Hopkins University School of Medicine, Baltimore, USA. June 2007
- Novartis Institute of Biomedical research (NIBR), Boston, USA, in June 2008
- Institute of Genomics and Integrative Biology (IGIB), New Delhi, India in December 2008
- National Institute of Immunology (NII), New Delhi, India, in December 2008
- Indian Institute of Chemical Technology (IICT), Hyderabad, India, December 2008
- Center for Cellular and Molecular Biology (CCMB), Hyderabad, India, in December, 2008
- Indian Institute of Chemical Biology (IICB), Kolkata, India, in December 2008.
- Indian Statistical Institute (ISI), Kolkata, India, in December 2008
- Calcutta Consortium for Human Genetics lecture, Kolkata University, Kolkata, India. July 2010
- Indian Institute of Cultivation of Sciences (IACS), Kolkata, India, in June 2011
- Indian Institute of Technology (IIT), Guwahati, Assam, India, September, 2011
- Bengal Engineering and Science University (BESU), Kolkata, February, 2013
- Johns Hopkins University (JHU) School of Medicine, Baltimore, USA, April 2013
- Institute of Bioinformatics (IOB), Bangalore, India, March 2014

**List of publications:** <http://scholar.google.co.in/citations?hl=en&user=pnxBJKsAAAAJ>

<b>Total number of peer reviewed publications</b>	<b>23</b>
<b>Total number of citations till date</b>	<b>2268</b>
<b><i>h</i>-index</b>	<b>17</b>
<b>Highest number of citations on a single publication</b>	<b>868</b>

### Corresponding senior authored research papers:

1. Biswas NK, Chandra V, Sarkar-Roy N Das T, Bhattacharya RN, Tripathy LN, Basu SK, Kumar S, Das S, Chatterjee A, Mukherjee A, Basu P, Maitra A, Chattopadhyay A, Basu A and Dhara S (2015) Variant allele frequency enrichment analysis *in vitro* reveals sonic hedgehog pathway to impede sustained temozolomide response in GBM. *Scientific Reports*, Posted online, | 5 : 7915 | DOI: 10.1038/srep07915 (First two authors contributed equally to this work)
2. Chandra V, Das T, Gulati P, Biswas NK, Rote S, Chatterjee U, Ghosh SN, Deb S, Saha SK, Chowdhury AK, Ghosh S, Rudin CM, Mukherjee A, Basu A and Dhara S (2015) Hedgehog signaling pathway is active in GBM with GLI1 mRNA expression showing a single continuous distribution rather than discrete high/low clusters. *PlosONE* | DOI:10.1371/journal.pone.0116390 March 16, 2015 (First three authors contributed equally to this work)

### Single authored book chapter:

3. **Dhara S.** (2008). Tumor Biology. Textbook of Molecular Imaging in Oncology. Pomper, M.G., Ed. New York: Taylor & Francis, pp. 1-26.

### First authored research papers:

4. Di Cello FP, Dhara S, Hristov AC, Kowalski J, Elbahloul O, Hillion J, Roy S, Meijerink JPP, Winter SS, Larson RS, Huso DL, and Resar LMS (2013) Inactivation of the *Cdkn2a* locus cooperates with *HMGAI* to drive T-cell leukemogenesis. *Leukemia & Lymphoma*, Posted online on January 11, 2013. (First two authors contributed equally to this work)
5. Hillion J, Dhara S, Sumter TF, Mukherjee M, Turkson J, Jove R, Bhattacharya R, Elbahloul O, Resar LMS. (2008) The HMG-I-STAT3 axis: An Achilles heel for human lymphoid leukemia? *Cancer Res.* 68:10121-10127. (First three authors contributed equally to this work)
6. Feldmann G, Dhara S, Fendrich V, Bedja D, Beaty R, Mullendore M, Karikari C, Alvarez H, Iacobuzio-Donahue C, Jimeno A, Gabrielson KL, Matsui W, Maitra A. (2007). Blockade of Hedgehog signaling inhibits pancreatic cancer invasion and metastases: A new paradigm for combination therapy in solid cancers. *Cancer Res.* 67: 2187-2196. (First two authors contributed equally to this work)
7. **Dhara S, Lalitkumar PGL, Sengupta J, Ghosh D.** (2001). Immunohistochemical localization of insulin-like growth factor-I and -II at the primary implantation site of the rhesus monkey. *Mol. Hum. Reprod.* 7: 365-371.

### Review Article:

8. Winnard PT, Pathak, AP, **Dhara S**, Cho SY, Raman V, Pomper MG. (2008) Molecular imaging of metastatic potential. *J Nucl Med.* 49(Supl. 2):96S- 112S.

**Contributing authored research papers:**

9. Shim JS, Matsui Y, Bhat S, Nacev BA, Xu J, Bhang HE, **Dhara S**, Han KC, Chong CR, Pomper MG, So A, Liu JO. (2011). Effect of nitroxoline on angiogenesis and growth of human bladder cancer. *J Natl Cancer Inst.* 102: 1855-1873.
10. Hillion J, Wood LJ, Mukherjee M, Bhattacharya R, Di Cello FP, Kowalski J, Elbahlou O, Poirier J, Rudin CM, **Dhara S**, Belton A, Joseph B, Zucker S, Resar LMS (2009). Upregulation of MMP-2 by HMGA1 Promotes Transformation in Undifferentiated, Large Cell Human Lung Cancer. *Mol. Cancer Res.* 11:1803-1812.
11. Chen Y, **Dhara S**, Byun Y, Pullambhatla M, Mease RC, Pomper MG. (2009) A Low Molecular Weight PSMA-Based Fluorescent Imaging Agent for Cancer. *Biochem. Biophys. Res. Com.* 390:624-629.
12. Feldmann G, Habbe N, **Dhara S**, Bisht S, Alvarez H, Fendrich V, Beaty R, Mullendore M, Karikari C, Bardeesy N, Oullette MM, Yu W, Maitra A. (2008) Hedgehog inhibition with cyclopamine prolongs survival in a genetically engineered mouse model of pancreatic cancer. *Gut* 57, 1420-1430.
13. Tesfaye A, Di Cello F, Hillion J, Ronnett BM, Elbahaloul O, Ashfaq R, **Dhara S**, Prochownik E, Tworkoski K, Reeves R, Roden R, Ellenson LH, Huso DL, Resar LM. (2007). The high-mobility group A1 gene up-regulates cyclooxygenase 2 expression in uterine tumorigenesis. *Cancer Res.* 67: 3998-4004. (First three authors contributed equally to this work)
14. Bonde P, Sui G, **Dhara S**, Wang, J., Broor, A., Kim, I.F., Wiley, J.E., Marti, G., Ferguson, M., Duncan, M., Jaffee, E.M., Montgomery, E.A., Maitra, A., Harmon, J.W. (2007). Cytogenetic characterization and gene expression profiling in the rat reflux induced esophageal tumor model. *J Thorac. Cardiovasc. Surg.* 133: 763-769.
15. Sui G, Bonde P, **Dhara S**, Broor A, Wang J, Marti G, Feldmann G, Duncan M, Montgomery, E, Maitra A, Harmon JW. (2006). Epidermal Growth Factor Receptor and Hedgehog Signaling Pathways Are Active in Esophageal Cancer Cells From Rat Reflux Model. *J. Surg. Res.* 134: 1-9.
16. Martin ST, Sato N, **Dhara S**, Hustinx SR, Abe T, Maitra A, Hruban RH, Goggins M. (2005). The Human Hedgehog Interacting Protein gene, HHIP, is aberrantly methylated in pancreatic cancer and is a mediator of hedgehog pathway activity in pancreatic carcinogenesis. *Cancer Biol. Ther.* 4:728-733.
17. Hansel DE, **Dhara S**, Huang RC, Ashfaq R, Deasel M, Shimada Y, Bernstein HS, Harmon J, Brock M, Forastiere A, Washington MK, Maitra A, Montgomery E. (2005). CDC2/CDK1 Expression in Esophageal Adenocarcinoma and Precursor Lesions Serves as a Cancer Progression Marker and Novel Drug Target. *Am. J. Surg. Pathol.* 29: 390-399.

18. Prasad N, Biankin AV, Fukushima N, Maitra A, **Dhara S**, Elkahloun AG, Hruban RH, Goggins M, Leach SD. (2005). Gene Expression Profiles in Pancreatic Intraepithelial Neoplasia Reflect the Effects of Hedgehog Signaling on Pancreatic Ductal Epithelial Cells. *Cancer Research* 65: 1619-1626.
19. Karhadkar SS, Bova SG, Abdallah N, **Dhara S**, Gardner D, Maitra A, Isaacs JT, Berman DM, Beachy PA. (2004). Hedgehog signaling in prostate regeneration, neoplasia, and metastasis. *Nature* 431: 707-712.
20. Parker AR, Leonard CP, Hua L, Francis RO, **Dhara S**, Maitra A, Eshleman JR. (2004). A subgroup of microsatellite stable colorectal cancers has elevated mutation rates and different responses to alkylating and oxidizing agents. *British Journal of Cancer* 90: 1666-1671.
21. Ghosh D, Sharkey AM, Charnock-Jones DS, Dhawan L, **Dhara S**, Smith SK, Sengupta J. (2000). Expression of vascular endothelial growth factor (VEGF) and placenta growth factor (PlGF) in conceptus and endometrium during implantation in the rhesus monkey. *Mol. Hum. Reprod.* 6: 935-941.
22. Ghosh D, **Dhara S**, Kumar A, Sengupta J. (1999). Immunohistochemical localization of receptors for progesterone and estradiol- 17b in the implantation site of the rhesus monkey. *Human Reproduction.* 14: 505-514.
23. Ghosh D, Nayek NR, Lalit Kumar PGL, **Dhara S**, Sengupta J. (1997). Hormonal requirement for blastocyst implantation and a new approach for anti-implantation strategy. *Indian J. Physiol. Pharmacol.* 41: 101-108.

**Abstracts presented in international meetings (Selected abstracts only)**

1. Biswas, N.K., Roy, N.S., Chandra, V., Das, T., Bhattacharya, R.N., Tripathy, L.N., Basu, S.K., Mukherjee, A., Basu, P., Maitra, A., Basu, A., and **Dhara, S.** (2013) Genetic mutations associated with Temozolomide induced cellular senescence in GBM neurospheres (AACR annual meeting, April-6-10, 2013, Wasington DC, USA) (First two authors have equally contributed to this work)
2. Das, T., Chatterjee, U., Ghosh, S.N., Deb, S., Saha, S.K., Gulati, P., Rote, S., Chandra, V., Mukherjee, M. and **Dhara, S.** (2013) An objective clustering of GBM patients to identify clinically relevant subgroups with hedgehog pathway activity ( AACR annual meeting, April 6-10, 2013 Wasington DC, USA).
3. **Dhara, S.**, Wang, H., Nimmagada, S., Mease, R. C., Bhujwalla, Z. M., Pomper, M.G. (2008). Synthesis and *In Vitro* Validation of a Radiolabeled Analog of Cyclopamine: A potential imaging agent for Hh-pathway (AACR annual meeting, April 12-16, 2008, San Diego, CA).
4. **Dhara, S.**, Iacobuzio, C., Maitra, A. (2006). Hedgehog Transcription Factor *Gli1* Induces An Invasive Phenotype In Immortalized Human Pancreatic Ductal Epithelial Cells. (AACR annual meeting, April 1-5, Washington, DC).

## RESEARCH STATEMENT

### Research background

I am a cancer biologist. My research interest has been cellular and molecular mechanisms underlying chemotherapy response in cancer. Why only some patients do while others do not respond to the same regimen of a therapy? Even after an initial response to a therapy why does a tumor relapse by developing an “acquired resistance”? Can we possibly make a non-responder patient respond or can we overcome chemotherapy resistance? These are the burning questions that I am currently pursuing. My basic training of biology was in the area of Human Physiology. The extensive cellular transformation of maternal endometrium at the embryo-endometrial interface – a well-studied model of cellular transformation under normal physiologic conditions was my Ph. D. thesis <sup>1</sup> – intrigued me towards understanding cancer biology. Therefore, in the following stages of academic career I decided to continue my research on cancer biology. My five years of postdoctoral training followed by a short period of research faculty appointment at the Johns Hopkins University, Baltimore, USA, I studied role of sonic hedgehog (Hh) signaling pathway, a developmentally important signaling pathway, as a therapeutic target in cancer. Here for the first time we demonstrated the pivotal role of the Hh-pathway in cancer metastasis – first in prostate cancer <sup>2</sup> and then in pancreatic cancer <sup>3</sup> we showed inhibition of the Hh-pathway could abrogate metastasis in preclinical mouse models of human tumor xenografts. I also co-authored several other papers on this pathway <sup>4-7</sup>. Then I studied the role of chromatin architectural protein HMG A1 in leukemia. We have shown HMG-STAT3 axis as an Achilles heel in human leukemia <sup>8,9</sup> and could be a potential therapeutic target. Lastly, we synthesized a radio-iodinated (<sup>125</sup>I) analog of cyclopamine, the classical pharmacological inhibitor of the Hh-pathway, in order to image this pathway *in vivo* in preclinical mouse tumor xenograft models. Our objective was to develop a potential imaging agent, which could be utilized for clinical stratification of patients in therapies with the Hh-pathway inhibitor drugs. We found the compound to be highly lipophilic, therefore could not be used *in vivo* in animals for imaging despite a specific interaction with Hh-positive cells *in vitro*. However, while finishing my 5<sup>th</sup> year of postdoctoral training one medulloblastoma (MB) case study that was conducted at the Johns Hopkins neuro-oncology clinic changed my whole perception of research on cancer chemotherapy. A 26 years old boy with MB had extensive metastasis spreads all over his body. The clinicians identified him as a “terminal case” and therefore recruited him in a clinical trial with Hh-pathway inhibitor GDC 0449. He had an amazing initial response with the drug, got almost cured in two months, but the disease relapsed and the poor boy died after another three months. Result of this trial was published in NEJM 2009 <sup>10</sup>. It was further investigated and was found that the relapsed lesions following drug treatment contained an additional non-synonymous mutation (D473H) in the drug target (SMO receptor) which completely abolished the drug binding to the target. That mutation was not detected in the lesions before the drug treatment. This was independently published in Science 2009 <sup>11</sup>. So, one mutation changed the whole scenario – from a grand success to a depressing failure. We do not know if that specific mutation was preexistent in a rare clone hidden somewhere within the heterogeneous clonal pool of the tumor, which enriched upon drug treatment, or newly developed by the drug treatment itself. But this intrigued me to extend my future research career towards understanding the underlying mechanisms of developing chemoresistance in cancer. In April 2010 I joined National Institute of Biomedical Genomics (NIBMG), a newly forming autonomous institution in India. Here as an independent researcher I wanted to identify genome wide mutations in tumor cells that are taking place after chemotherapy *in vitro* and also *in vivo* by utilizing the strength of advanced whole genome deep sequencing technologies.

## Current research focus

*Understanding chemotherapy response in cancer with the perspective of intra-tumor heterogeneity:* My past research experience had made me to realize that cancer chemoresistance was a bigger hurdle in the war against cancer, than even developing an anti-cancer drug. I pursue my current research on cancer chemotherapy, precisely to understand the basic mechanisms of chemoresistance with a perspective of intra-tumor heterogeneity. Growing body of evidence suggests clonal heterogeneity of cancer cells, *in vivo* as well as *in vitro* – be it genetic or non-genetic heterogeneity – to be playing a pivotal role in chemotherapy response<sup>12, 13</sup>. Genetic heterogeneity assumes every individual clone to have “signature set of mutations”. Therefore, changes in clonal predominance following an exposure to a chemotherapeutic drug are supposed to be reflected in the mutation spectrum of the cells (the heterogeneous clonal pool). Change of mutation spectrum before and after a drug treatment can be characterized by deep DNA sequencing technologies – as enriching frequency of mutations on each genetic locus – as detected by locus-by-locus comparison of variant allele frequencies (VAFs) before and after exposure to a chemotherapeutic drug<sup>14</sup>. By exploring this model of VAF analysis *in vitro*, recently we have established a role of the Hh-pathway to impede temozolomide chemotherapy response in glioblastoma multiforme<sup>15</sup>. Further, while stratifying GBM patients on the basis of the Hh-pathway activity we observed and published<sup>16</sup> the Hh-transcription factor GLI1 mRNA expression in GBM showing a single continuous distribution rather than high/low- mRNA expression clusters, unlike medulloblastoma. As one of the major projects currently we are trying to define a better method of clinical stratification of GBM patients in therapies with the Hh-pathway inhibitor drugs. Also, through an agnostic approach, by high throughput deep sequencing and microarray technologies, we are trying to understand the biological basis of chemotherapy response in malignant diseases like GBM and Head & Neck cancers. A more detailed and structured research proposal with Specific Aims and appropriate study design could also be available upon request.

## Essential infrastructure

**a)** Collaborative programs with Surgeons, Pathologists and Medical Oncologist in a hospital set-up. **b)** Tissue culture facility with fluorescent microscopy, **c)** flow cytometry facility, **d)** deep sequencing (optional) facility, **e)** immunocompromised mouse facility and **f)** approximately 500 sqft of laboratory space.

## References

- 1 Dhara, S., Lalitkumar, P. G., Sengupta, J. & Ghosh, D. Immunohistochemical localization of insulin-like growth factors I and II at the primary implantation site in the Rhesus monkey. *Molecular human reproduction* **7**, 365-371 (2001).
- 2 Karhadkar, S. S. *et al.* Hedgehog signalling in prostate regeneration, neoplasia and metastasis. *Nature* **431**, 707-712 (2004).
- 3 Feldmann, G. *et al.* Blockade of hedgehog signaling inhibits pancreatic cancer invasion and metastases: a new paradigm for combination therapy in solid cancers. *Cancer research* **67**, 2187-2196 (2007).
- 4 Feldmann, G. *et al.* Hedgehog inhibition prolongs survival in a genetically engineered mouse model of pancreatic cancer. *Gut* **57**, 1420-1430 (2008).
- 5 Sui, G. *et al.* Epidermal growth factor receptor and hedgehog signaling pathways are active in esophageal cancer cells from rat reflux model. *The Journal of surgical research* **134**, 1-9 (2006).



- 6 Martin, S. T. *et al.* Aberrant methylation of the Human Hedgehog interacting protein (HHIP)  
gene in pancreatic neoplasms. *Cancer biology & therapy* **4**, 728-733 (2005).
- 7 Prasad, N. B. *et al.* Gene expression profiles in pancreatic intraepithelial neoplasia reflect the  
effects of Hedgehog signaling on pancreatic ductal epithelial cells. *Cancer research* **65**, 1619-  
1626 (2005).
- 8 Di Cello, F. *et al.* Inactivation of the Cdkn2a locus cooperates with HMGA1 to drive T-cell  
leukemogenesis. *Leukemia & lymphoma* **54**, 1762-1768 (2013).
- 9 Hillion, J. *et al.* The high-mobility group A1a/signal transducer and activator of transcription-3  
axis: an achilles heel for hematopoietic malignancies? *Cancer research* **68**, 10121-10127 (2008).
- 10 Rudin, C. M. *et al.* Treatment of medulloblastoma with hedgehog pathway inhibitor GDC-0449.  
*The New England journal of medicine* **361**, 1173-1178 (2009).
- 11 Yauch, R. L. *et al.* Smoothed mutation confers resistance to a Hedgehog pathway inhibitor in  
medulloblastoma. *Science (New York, N.Y)* **326**, 572-574 (2009).
- 12 Marusyk, A., Almendro, V. & Polyak, K. Intra-tumour heterogeneity: a looking glass for cancer?  
*Nature reviews* **12**, 323-334 (2012).
- 13 Patel, A. P. *et al.* Single-cell RNA-seq highlights intratumoral heterogeneity in primary  
glioblastoma. *Science (New York, N.Y)* **344**, 1396-1401 (2014).
- 14 Aparicio, S. & Caldas, C. The implications of clonal genome evolution for cancer medicine. *The  
New England journal of medicine* **368**, 842-851 (2013).
- 15 Biswas, N. K. *et al.* Variant allele frequency enrichment analysis in vitro reveals sonic hedgehog  
pathway to impede sustained temozolomide response in GBM. *Scientific Reports* | 5: 7915 | DOI:  
10.1038/srep07915 (2015).
- 16 Chandra, V. *et al.* Hedgehog signaling pathway is active in GBM with GLI1 mRNA expression  
showing a single continuous distribution rather than discrete high/low clusters. *PloS one (in  
press)* (2015).

## TEACHING STATEMENT

### TEACHING BACKGROUND

**Teaching assistant during graduate studies:** While in my graduate studies I served for 3 years to teaching. I took demonstrative practical classes on physiology of blood cells to the 1<sup>st</sup> year medical/nursing graduate students of AIIMS for their Physiology course work. It was 6 contact hours per day, once a week for a whole semester. My responsibilities included teaching the physiology and pathophysiology of blood and bone marrow cells to the students with PowerPoint presentation followed by demonstration of staining and identification of the specific cells of blood and bone marrow under light microscope in the practical classes. It also included helping the concerned faculty members with class assessments and scoring credits.

**Senior Demonstrator:** Later, I was selected and appointed as a Senior Demonstrator (equivalent to an Instructor position) by the Department of Physiology, AIIMS. The job responsibilities included full-fledged teaching and assessment of medical/nursing/graduate students for their theory and practical classes in Human Physiology. It was similar to the teaching assistant work that I had done before but with lot more responsibilities. I continued doing this job for 2 years from September 2000 till August 2002, when I left for my postdoctoral training in the USA.

**Teaching Cancer Biology for the Ph. D. coursework of NIBMG:** Routinely, from last 4 years I have been taking Cancer Biology classes for the Ph. D. coursework of NIBMG. My cancer biology course is total of 30 contact hours in one semester. I teach the students the whole of cancer biology, giving them an overview of the disease from a cell biologist's perspective. The class is structured on the basis of a book chapter that I had written (single authored) on Tumor Biology, that is a lead chapter in "Textbook of Molecular Imaging in Oncology" *Taylor & Francis, New York, (2008)*. It encompasses some of the basic aspects of cell biology, developmental biology along with cancer genetics, cancer biology and principles of cancer therapy – starting with the historical perspective to present day's research. Being a cancer researcher myself I could give the students some glimpses of the pertinent recent discoveries in the field. The purpose of this class is to make the students feel interested in cancer research, to provide them with a solid foundation of knowledge in cancer biology and also to help them picking up their independent research career path in the field of cancer.

**Mentoring:** My reputation as a researcher, educator and collaborator has resulted in a stream of students from within state and elsewhere who have sought me as a mentor. I have been an effective mentor for postdoctoral fellows, graduate students, undergraduate students, and even high school students. My job responsibilities include mentoring graduate students, taking regular classes for graduate training program along with carrying on my own independent research. Currently, I am supervising a Ph. D. student who is completing the third year of his thesis under my direct mentorship. The second one is a Research Assistant, who is helping us with bioinformatics analyses of the high throughput genomic/transcriptomics data. I have also mentored a Young Biotechnology (YBA) Fellow. Currently he is in the Ph. D. Program of Weill Cornell Medical College, Cornell University, NY, USA. The bright

careers of my mentees make me feel proud and give me a moral incentive to be a good teacher. I have also mentored summer trainees during my postdoctoral fellowship at the Johns Hopkins University.

**Outreach programs and guest lectures to high school students:** In addition to teaching medical graduate/ nursing/ Ph. D students I have also taught High school students – in special outreach programs to make them feel interested about scientific research as their future career. I could have not realized the power of young minds, the enormous potential and the enthusiasm that they have, if I had not spent those few hours with them. The naïve, yet brilliant questions that the bright young high school students ask that always impressed me more than ever. Teaching them was fun.

### **TEACHING INTEREST**

As a faculty member I would be interested in applying my teaching principles to a wide range of graduate and undergraduate courses in the general areas of Cell Biology, Cancer Biology and also some basic Biochemistry. I would like to pursue the development of more specialized courses on Cancer Experimental therapeutics, *in vitro* and *in vivo* (mouse) models for pharmaceutical drug discovery and development along with the current state of the art genomics and bioinformatics for the development of interdisciplinary cutting-edge courses.

### **TEACHING PHILOSOPHY**

A teacher who can inculcate curiosity and inquisitiveness in the student's mind is the best teacher. In all my teaching classes, my ultimate goal always has been to foster student's passions and curiosity. I strongly believe that every individual student can have their own skill and individual ways of thinking and assimilating a subject. Only thing that is required is to make them feel attracted and interested towards it, so that they start believing the enormous power and potential of their unexplored young minds. I always try my best to clear their visions with the wide range of experience that I have received from my teachers, the best of the bests, the great teachers and the leaders of the field where I had my training done. Clarity of vision makes students more motivated towards a subject that interests them.



## OPEN

SUBJECT AREAS:  
CNS CANCER  
CANCER GENOMICSReceived  
22 September 2014Accepted  
22 December 2014Published  
21 January 2015Correspondence and  
requests for materials  
should be addressed to  
S.D. (sd1@nibmg.ac.  
in) or S.D.  
(Surajit\_dhara@  
hotmail.com)\* These authors  
contributed equally to  
this work.

# Variant allele frequency enrichment analysis *in vitro* reveals sonic hedgehog pathway to impede sustained temozolomide response in GBM

Nidhan K. Biswas<sup>1\*</sup>, Vikas Chandra<sup>1\*</sup>, Neeta Sarkar-Roy<sup>1</sup>, Tapojyoti Das<sup>1</sup>, Rabindra N. Bhattacharya<sup>2</sup>, Laxmi N. Tripathy<sup>3</sup>, Sunandan K. Basu<sup>3</sup>, Shantanu Kumar<sup>1</sup>, Subrata Das<sup>1</sup>, Ankita Chatterjee<sup>1</sup>, Ankur Mukherjee<sup>1</sup>, Priyadarshi Basu<sup>1</sup>, Arindam Maitra<sup>1</sup>, Ansuman Chattopadhyay<sup>4</sup>, Analabha Basu<sup>1</sup> & Surajit Dhara<sup>1</sup><sup>1</sup>National Institute of Biomedical Genomics, Kalyani, West Bengal 741251, India, <sup>2</sup>AMRI Hospitals, JC-16 Salt Lake City, Kolkata 700098, India, <sup>3</sup>Medica Superspeciality Hospital, 127 Mukundapur, Kolkata 700099, India, <sup>4</sup>University of Pittsburgh, 3550 Terrace Street, Pittsburgh, PA 15261, USA.

Neoplastic cells of Glioblastoma multiforme (GBM) may or may not show sustained response to temozolomide (TMZ) chemotherapy. We hypothesize that TMZ chemotherapy response in GBM is predetermined in its neoplastic clones via a specific set of mutations that alter relevant pathways. We describe exome-wide enrichment of variant allele frequencies (VAFs) in neurospheres displaying contrasting phenotypes of sustained versus reversible TMZ-responses *in vitro*. Enrichment of VAFs was found on genes ST5, RP6KA1 and PRKDC in cells showing sustained TMZ-effect whereas on genes FREM2, AASDH and STK36, in cells showing reversible TMZ-effect. Ingenuity pathway analysis (IPA) revealed that these genes alter cell-cycle, G2/M-checkpoint-regulation and NHEJ pathways in sustained TMZ-effect cells whereas the lysine-II&V/phenylalanine degradation and sonic hedgehog (Hh) pathways in reversible TMZ-effect cells. Next, we validated the likely involvement of the Hh-pathway in TMZ-response on additional GBM neurospheres as well as on GBM patients, by extracting RNA-sequencing-based gene expression data from the TCGA-GBM database. Finally, we demonstrated TMZ-sensitization of a TMZ non-responder neurosphere *in vitro* by treating them with the FDA-approved pharmacological Hh-pathway inhibitor vismodegib. Altogether, our results indicate that the Hh-pathway impedes sustained TMZ-response in GBM and could be a potential therapeutic target to enhance TMZ-response in this malignancy.

Glioblastoma multiforme (GBM) is a lethal malignancy of the central nervous system (CNS) showing dismal prognosis under the standard care of surgery, adjuvant radiotherapy and temozolomide (TMZ) chemotherapy<sup>1</sup>. Both radiotherapy and TMZ chemotherapy induce DNA damage in GBM neoplastic cells by means of generating double-strand breaks (DSB) and single-strand breaks (SSB) respectively. Ionizing radiation (IR) directly induces DSB and TMZ induces SSB by alkylating purine residues at the nucleotide positions of N-7, O-6 for Guanine (N-7-me-G, O-6-me-G) and N-3 for Adenine nucleotides (N-3-me-A), thus activating the base excision repair (BER) pathway<sup>2-5</sup>. Following alkylation, the damaged bases of the affected cells, are removed first by BER-glycosylase enzymes generating apurinic/aprimidinic (AP)-sites followed by AP-endonucleases (APE) to finally generate SSB. Eventually both SSB and DSB converge to elicit the final response through common DNA damage response (DDR) pathways, to determine the fate of the damaged cell, either a sustained terminal response phenotype like apoptosis/senescence or a reversible response phenotype like quiescence (transient cell cycle arrest to repair the damage)<sup>4,5</sup>. Despite considerable knowledge of the molecular mechanism(s) of TMZ-response in GBM, it remains unclear why some cells respond to TMZ by showing a sustained effect such as apoptosis/cellular senescence while others do not.

A growing body of evidence *in vitro* as well as *in vivo* suggests clonal heterogeneity of cancer cells (genetic or non-genetic heterogeneity), to play a pivotal role in chemotherapy response<sup>6-10</sup>. We demonstrate here a plausible

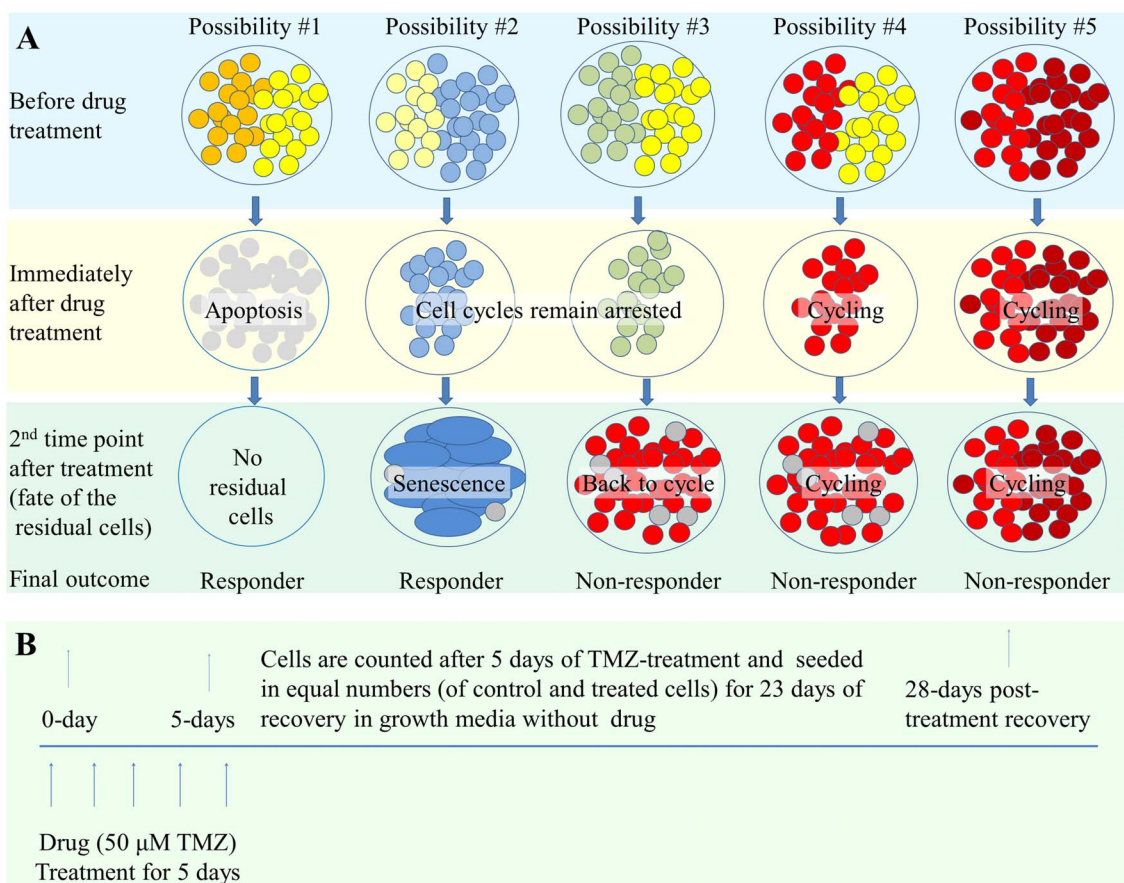


**Figure 1** | (A) Schematic diagram of a model to explain TMZ-response in GBM neoplastic cells on the perspective of clonal heterogeneity. (B) The experimental design for TMZ-treatment and post-treatment recovery of GBM neurospheres *in vitro* to address this hypothetical model of TMZ-response.

model to explain TMZ-response of GBM neoplastic cells with the perspective of clonal heterogeneity. The most desirable outcome of GBM heterogeneous clones exposed to the maximum clinically achievable dose of TMZ<sup>11</sup> is induction of apoptosis and death. However, only a proportion of these clones induce apoptosis as an instant effect of TMZ-treatment. The residual clones, either show sustained growth arrest followed by induction of cellular senescence, or are non-responders. We sought to identify the genetic basis of these residual clones showing either a reversible drug-effect or a sustained drug-effect in response to TMZ. We explore here genetic heterogeneity of GBM neoplastic cells to estimate clonal enrichment in response to TMZ-treatment *in vitro*. Genetic heterogeneity assumes every individual clone to have a “signature set of mutations”<sup>9,12</sup>. Therefore, changes in clonal predominance after an exposure to chemotherapeutic drugs (*in vitro* or *in vivo*) will be reflected in the mutation spectrum of the cells as detected by comparison of variant allele frequencies (VAFs) before and after drug exposure<sup>13</sup>.

We hypothesize TMZ-response to be predetermined in clones of GBM neoplastic cells with a specific set of mutations altering relevant pathways. In order to test the hypothesis, we developed an *in vitro* TMZ-treatment and post-treatment recovery model with GBM patient-derived neurospheres in our laboratory following a model previously described by Mihaliak *et al.*<sup>14</sup>. First we identified two clinical patients, one a TMZ-responder still living as of publication (for more than 38 months) and the other a non-responder who died within 3 months of surgery. Then we isolated neoplastic cells from surgically resected tumors from both patients, grew them in culture as neurospheres, exposed them to the maximum clinically achievable dose of TMZ (50  $\mu$ M)<sup>11</sup> *in vitro* for 5 days, and then allowed them to grow for 28 days without the drug. Although the responder patient-derived neurosphere did not show induction of apoptosis in response

to TMZ, almost all residual cells underwent TMZ-induced cellular senescence (TICS). Conversely, the non-responder patient-derived neurosphere underwent extensive apoptosis as an initial response to TMZ-treatment and the residual cells readily resumed proliferation upon drug withdrawal. These contrasting phenotypes were repeatedly observed in the two neurospheres irrespective of their cellular passages. In order to detect these two contrasting TMZ-responsive residual cells, we performed whole exome deep sequencing analysis of both the neurospheres at 3 different time points: before TMZ-treatment, after TMZ-treatment and after 28 days of post-treatment recovery *in vitro*. We then estimated exome-wide enrichment of VAFs and used Ingenuity pathway analysis (IPA) software to reveal the relevant pathways, as altered by the genes where VAFs were enriched in response to TMZ. Sonic hedgehog (Hh) pathway, one of the four pathways determined by our analysis, was significantly hyper-activated in cells showing reversible drug-effect. We then verified the likely involvement of the Hh-pathway by phenotypically clustering additional neurospheres in our repository with MGMT expression and TMZ-response *in vitro*. Finally, we demonstrated TMZ-sensitization of a TMZ-non-responder neurosphere *in vitro* by treatment with an FDA approved pharmacological Hh-pathway inhibitor vismodegib<sup>15,16</sup>.

## Results

**A plausible model of chemotherapy response in GBM based on clonal heterogeneity.** When GBM neoplastic cells are exposed to the chemotherapeutic drug TMZ, the first theoretical possibility (possibility # 1 in Fig. 1A) is that all cells undergo apoptosis and die, leaving no residual cells. Another extreme is possibility # 5 (Fig. 1A), nothing happens to the cells and they keep cycling. The other possibilities are partial apoptosis (possibilities #2, #3 and #4 in Fig. 1A). Under these



conditions, the residual cells following drug withdrawal may either show cell-cycle arrest (possibilities #2 and #3) or they may keep cycling (possibility #4). The cells which initially show cell-cycle arrest may either undergo a terminal differentiation by inducing cellular senescence resulting sustained response after the drug withdrawal (possibility #2) or may show reversible drug-effect by going back to the cell-cycle again (possibility #3). We provide evidence for possibilities #2 and #3 as a result of two GBM patient-derived neurospheres which repeatedly showed sustained versus reversible response to TMZ-treatment *in vitro*, irrespective of their cellular passages. Our experimental design of TMZ-treatment and post-treatment recovery (Fig 1B) was modified from Mihaliak *et al.*<sup>14</sup>.

**Clinical response of the two lead GBM patients.** Clinical responses of the two lead GBM patients, from whom we identified the phenotypes, are briefly described here. The first patient A49910 was a TMZ-responder. Recurrence of the tumor along the periphery of the surgically resected area was revealed in this patient after the 2<sup>nd</sup> cycle of chemotherapy (Fig. 2c). This mass appeared to decrease in size as observed in the follow-up scans done 5 months later after the completion of all the 6 cycles of TMZ chemotherapy (Fig. 2d). This is suggestive of good response to TMZ chemotherapy. The patient appeared to be doing well and free from clinical progression during follow-up visits for more than 38 months post-surgery. The second patient M45481 died in three months after surgery despite a similar treatment regimen.

**Development of GBM patient-derived neurospheres and MGMT analysis.** We isolated neoplastic cells from tumors of GBM patients at the time of surgery and grew them in culture as neurospheres. Altogether six neurospheres were developed from tumor biopsies of six GBM patients (including the two lead patients as described above). Relative values of MGMT mRNA expression (relative to GAPDH mRNA) from all six tumor biopsy tissues and corresponding tumor-derived neurospheres, as given in Figures 2e and 2f respectively, showed a very tight correlation (Pearson  $r = 0.9513$ ,  $p$ -value 0.0035). Henceforth, the isolated neurospheres will be referred as A49910, B0027, M45481, B0043, B0051 and B0048. MGMT expression in M45481 was significantly higher than that of A49910, both in tumor biopsy tissues ( $p$ -value 0.00243) and in the isolated neurospheres ( $p$ -value  $9.71128 \times 10^{-5}$ ).

**TMZ-treatment response of the isolated neurospheres *in vitro*.** All the *in vitro* TMZ-treatment experiments were done on the neurospheres A49910 and M45481 between passages 4–16. Results were consistent in the neurospheres irrespective of their cellular passages *in vitro*. To simulate the 28-day cycle of TMZ chemotherapy in patients we treated all of the isolated neurospheres with the maximum clinically achievable dose of TMZ (50  $\mu$ M) *in vitro* for 5 consecutive days and grew them for another 23 days without any drug intervention (post-treatment recovery). After 5 days, in A49910 viable cell count was  $54.6 \pm 22.9\%$  ( $p$ -value  $1.067 \times 10^{-5}$ ) and in M45481 it was  $32.3 \pm 6.6\%$  ( $p$ -value  $9.883 \times 10^{-7}$ ) compared to their

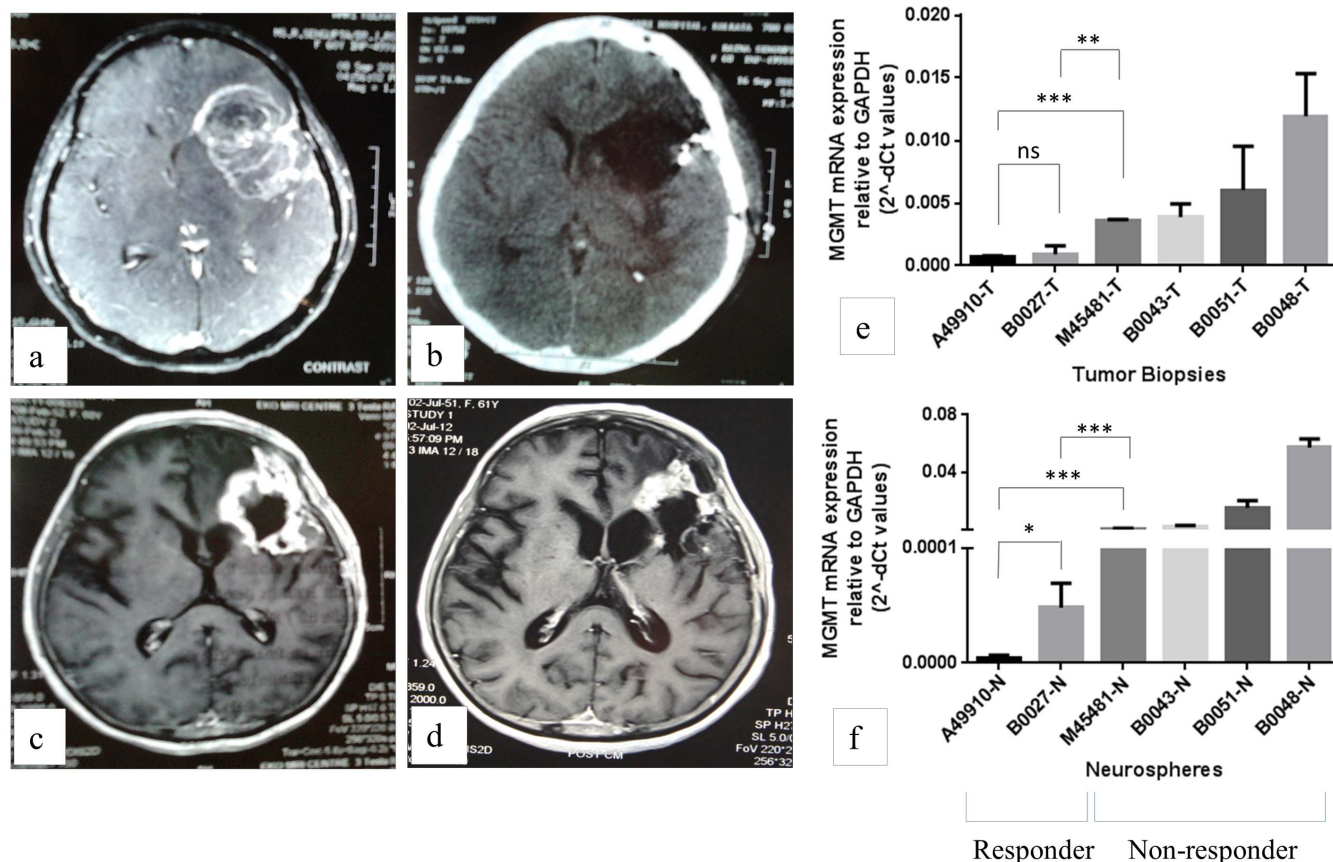


**Figure 2 | Radiological images of responder GBM patient A49910 and MGMT mRNA expressions of 6 GBM patient-derived tumor biopsy tissues and isolated neurospheres. (a),** Diagnostic MRI scan of the brain showing a space-occupying lesion (SOL) in insular cortex in A49910. **(b),** Postoperative CT scan showing gross total resection in A49910. **(c),** MRI scan image after the 2<sup>nd</sup> cycle of chemotherapy showing recurrence of the tumor in A49910. **(d),** Follow-up scan after 6 cycles of chemotherapy showing decrease in the size of the lesion in A49910. qRT-PCR estimation of MGMT mRNA expression relative to GAPDH mRNA expression in **(e),** GBM tumor biopsies and **(f),** in corresponding neurospheres isolated from the tumors. (\*  $p$ -value  $< 0.05$ , \*\*  $p$ -value  $< 0.01$  and \*\*\*  $p$ -value  $< 0.001$ ).

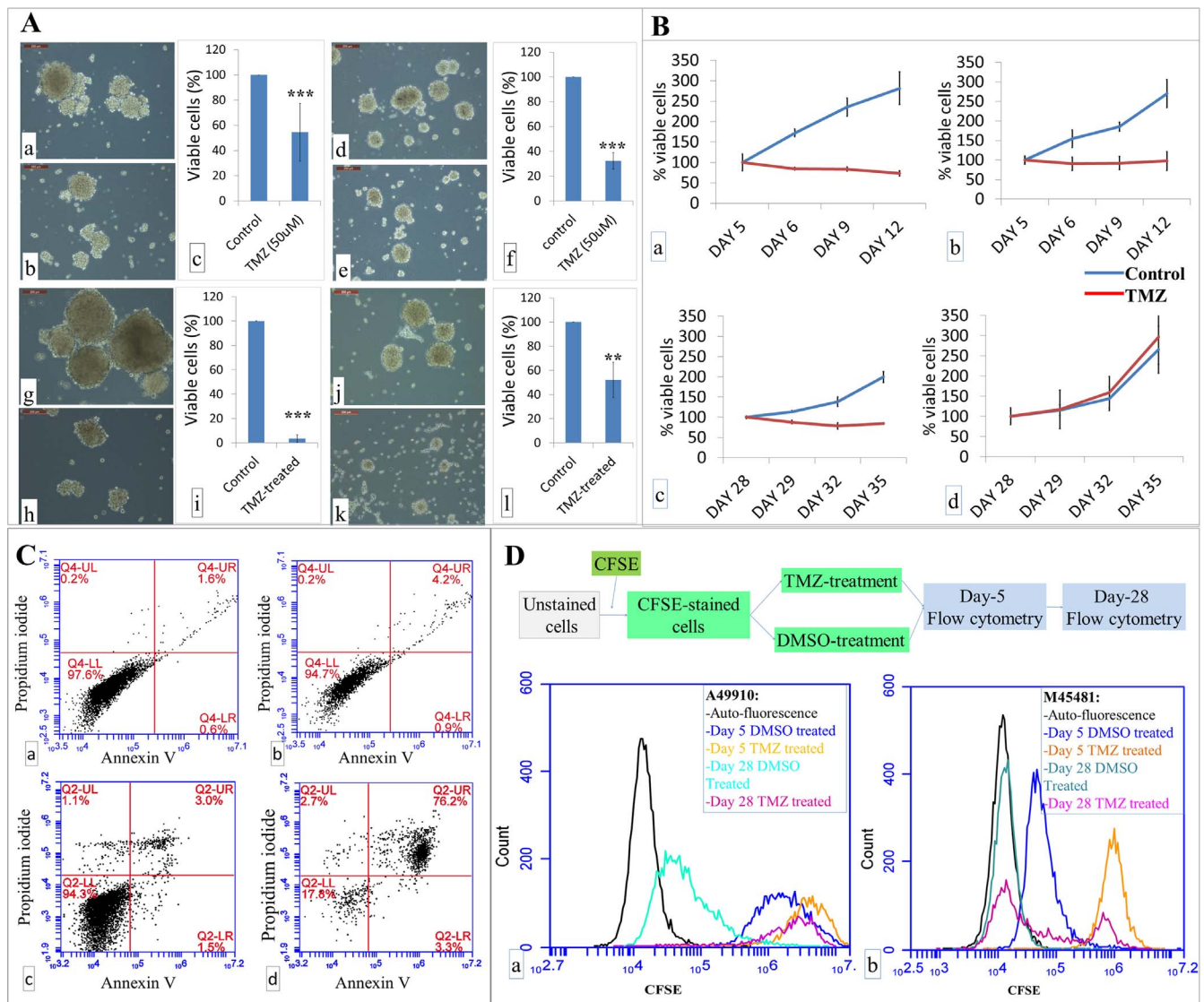


**Figure 3** | (A) Light microscopic images (200 μm bar) and viable cell count of the neurospheres following TMZ treatment and post-treatment recovery. (a), DMSO treated control and (b), 5 days TMZ-treated neurospheres in A49910. (c), % viable cells in A49910 with DMSO- and 5 days of TMZ-treatment. (d), DMSO-treated control and (e), 5 days TMZ-treated neurospheres in M45481. (f), % viable cells in M45481 with DMSO- and 5 days of TMZ-treatment. (g), DMSO-treated control and (h), 28 days of post-TMZ-treated neurospheres in A49910. (i), % viable cells of DMSO-treated controls and 28 days of post-TMZ-treated cells in A49910. (j), DMSO treated control and (k), 28 days post-TMZ-treated neurospheres in M45481. (l), % viable cells of DMSO-treated controls and 28 days of post-TMZ-treated cells in M45481. (\* p-value < 0.05, \*\* p-value < 0.01 and \*\*\* p-value < 0.001). (B) Growth curves (MTS assay) following 5 days of TMZ treatment and 28 days of post-treatment recovery. (a), A49910 DMSO-treated control and 5 days of TMZ-treated cells; (b), M45481 DMSO-treated control and 5 days of TMZ-treated cells; (c), A49910 DMSO-treated control and 28 days of post-TMZ-treated cells; (d), M45481 DMSO-treated control and 28 days of post-TMZ-treated cells. (C), flow cytometry analysis of apoptosis using annexin V and propidium iodide staining. (a), DMSO-treated A49910 cells, (b), 5 days of TMZ-treated A49910 cells, (c), DMSO treated M45481 cells and (d), 5 days of TMZ-treated M45481 cells. (D) Tracking cell division by CFSE staining. (a), growth arrest of TMZ-treated A49910 cells at day 5 of treatment (yellow line) compared to corresponding DMSO-treated control (blue line). The TMZ-treated A49910 cells remained arrested till day 28 post-treatment recovery (pink line) while the DMSO-treated control cells proliferated (green line). (b), Growth arrest in TMZ-treated M45481 cells at day 5 of treatment (yellow line) compared to corresponding DMSO-treated controls (blue line). At day 28 post-treatment recovery one subpopulation of TMZ-treated M45481 cells showed growth arrest while other subpopulation proliferated (pink line) showing a staining intensity almost similar to their corresponding DMSO-treated control cells (green line).

corresponding DMSO-treated controls (as 100%) as shown in Figure 3A c and f. But after 28<sup>th</sup> day the viable cell count was  $3.5 \pm 3.2\%$  in A49910 (p-value  $1.231 \times 10^{-10}$ ) and  $52.1 \pm 14.6\%$  in M45481 (p-value 0.001117) suggesting sustained effect of the drug only in A49910, but not in M45481 (Fig 3A i and l). TMZ-treatment experiments *in vitro* were repeated 6 times on A49910 and 3 times on M45481 with technical replicates. Error bars were generated and

statistical significances (p-values) were calculated including all the independently repeated experiments as biological replicates.

**Growth curves of the neurospheres following TMZ-treatment and post-treatment recovery.** After 5 days of TMZ-treatment, both A49910 and M45481 cells showed significant growth inhibition compared to their respective DMSO-treated controls as shown in



Figures 3B a and b (p-values were 0.00028 for A49910 and 0.00191 for M45481 after 5 days of treatment). After 28<sup>th</sup> day of post-treatment recovery it was only the TMZ-treated cells of A49910 but not that of M45481 showed sustained growth retardation, as shown in Figures 3B c and d (p-values 0.00551 for A49910 and 0.35536 for M45481 after 28 days of post-treatment recovery). Error bars were generated from the triplicate OD values of each experiment. All the MTS assays were repeated at least 2 times for each cell types at their two independent passages and found consistent results.

**Apoptosis versus sustained growth arrest in response to TMZ-treatment.** We observed extensive apoptosis in M45481 cells, as shown by 76% annexin V and propidium iodide double positive cells (Fig. 3C d), in response to 5 days of TMZ-treatment, whereas in A49910 it was only 4.2% (Fig. 3C b). On the other hand, A49910 cells showed sustained growth arrest till 28<sup>th</sup> day even after the drug withdrawal after 5 days, but the residual cells of M45481 resumed proliferation upon withdrawal of the drug as demonstrated by CFSE (Carboxy Fluorescein Succinimidyl Ester) staining (Fig. 3D a and b respectively). Corroborating with MTS assay (as described above) CFSE staining clearly demonstrated growth arrests in both A49910 and M45481 cells after 5 days of TMZ-treatment but that growth arrest was sustained till 28<sup>th</sup> day only in TMZ-treated cells of A49910, not that of M45481 (pink lines in Figure 3D a and b respectively).

**TMZ-induced cellular senescence (TICS) *in vitro*.** Sustained growth arrest in A49910 is due to induction of cellular senescence as revealed by flattened cellular morphology and SA- $\beta$ -Gal staining. Morphologies at the single cellular levels as repeatedly observed in all the *in vitro* TMZ-treatment experiments are represented in Figure 4A. At day 5, qualitatively, there were no morphological differences observed between the TMZ-treated cells of A49910 (Fig. 4A e) and their corresponding DMSO treated cells (Fig. 4A a) but at day 28, large and flattened appearance was visible only in the TMZ-treated cells (Fig. 4A f) but not in the corresponding DMSO-treated cells (Fig. 4A b). Unlike A49910, at day-5, the TMZ-treated cells of M45481 (Fig. 4A g) were appearing slightly bigger than their corresponding DMSO-treated control cells (Fig. 4A c) but at day 28, both the TMZ-treated (Fig. 4A h) and the DMSO-treated (Fig. 4A d) cells appeared almost similar in sizes. By a qualitative SA- $\beta$ -Gal colorimetric staining, the TMZ-treated A49910 cells showed intense blue cytoplasmic staining of SA- $\beta$ -Gal at day 28 post-treatment recovery (Fig. 4B f), suggesting induction of cellular senescence by TMZ-treatment. Some degree of blue cytoplasmic staining was also observed in DMSO-treated control cells of A49910 at day 28, but unlike the TMZ-treated cells, the control cells did not show any big and flat morphology. However, M45481 cells did not show any SA- $\beta$ -Gal staining, neither after 5 days of TMZ-treatment (Fig. 4B c vs. g) nor after 28 days of post-treatment recovery (Fig. 4B d vs. h).

**Enrichment of VAFs in response to TMZ-treatment and post-treatment recovery.** From the phenotypes we see the residual cells of A49910 showing sustained growth arrest and TICS in response to TMZ-treatment *in vitro*. On the other hand, the residual cells of M45481 resume proliferation readily after the drug withdrawal, despite showing extensive apoptosis as an initial response to TMZ-treatment *in vitro*. In order to detect the “specific set of mutations” in the residual cells of both the neurospheres following TMZ-treatment we analyzed the exome-wide enrichment of VAFs locus by locus in both the neurospheres at 3 different time points – before TMZ treatment (C5), 5 days after TMZ treatment (T5) and 28 days after post-treatment recovery (T28). Significantly (p-values < 0.01) altered VAFs showed biphasic trends of change with the first phase representing the comparisons between C5 to T5 and the second phase between T5 to T28 as shown in Figure 4C. In this way altogether 77 loci were identified in A49910, of them 45 were enriching. Similarly, 92 loci were identified in M45481 of them 51 were enriching. The

enriching VAFs are shown in red arrows in Figure 4C. Lists of all these loci are given in Supplementary Tables S17A and S17B. Detailed lists of the variant loci showing these trends of VAF enrichment are given in Supplementary Tables S2 through S14.

**Bioinformatic analyses of pathways by Ingenuity pathway analysis (IPA).** Next we detected the pathways altered by the genes on which the variant loci (mutations) were enriching in response to TMZ-treatment *in vitro*. As shown in Table 1 cell-cycle G2/M DNA damage checkpoint regulation and double strand break repair by non-homologous end joining (NHEJ) were the two pathways altered in A49910 by genes with enriching VAFs – by PRKDC, encoding for the catalytic subunit of the DNA-dependent protein kinase (DNA-PKCs), and by RPS6KA1, encoding for a member of the RSK (ribosomal S6 kinase) family of serine/threonine kinases respectively. Similarly, the pathways altered in M45481 by the genes with enriching VAFs were lysine degradation II, V, phenylalanine degradation IV and sonic hedgehog (Hh) signaling pathway – altered by AASDH gene encoding for 2-Amino adipic 6-Semialdehyde dehydrogenase enzyme and by STK36 gene encoding for an enzyme serine/threonine protein kinase 36 respectively. The selected list of genes where VAFs enriched  $\geq 70\%$  and/or the genes significantly altered relevant pathways as revealed by IPA are summarized in Table 1. The complete list of significantly altered pathways as revealed by IPA is given in Supplementary Table S16.

**Functional validation of increased Hh-pathway activity (in the residual cells) through TMZ-treatment and post-treatment recovery.** First by Sanger sequencing analysis we confirmed the presence of the variant locus of STK36 (Chromosome 2: 219557978 G to A) in M45481 but not in A49910 (Fig. 4D), taking two independent passages of each cell types. This mutation appeared to be novel. PolyPhen-2 prediction software showed it was a “deleterious” mutation (Supplementary Table S15) but we do not know at this moment how precisely this novel mutation on STK36 gene might be influencing the Hh-pathway activity in GBM. Therefore, we checked expressions of 11 canonical Hh-pathway component genes at three time points – before TMZ treatment, after TMZ treatment and after 28 days of post treatment recovery. As shown in Figure 4E a, mRNA expression of STK36 was found to be significantly increased in M45481 but not in A49910 cells upon TMZ-treatment. Significant increase in mRNA expressions was observed for the Hh-transcription factors GLI1, GLI2 and GLI3 upon TMZ-treatment and post-treatment recovery (Fig. 4E b, c, d). Similar patterns were also observed for SNAI1, as a bona fide downstream target of the Hh-pathway, and for MGMT, as a bona fide covariate of TMZ response in GBM (Fig. 4E e, f). These expression analyses were done in the neurospheres with biological replicates (at least 3 independently repeated experiments in each) as well as with the qRT-PCR technical replicates.

**Validation on additional neurospheres for the likely involvement of Hh-pathway in TMZ-response.** Next, we validated the likely involvement of Hh-pathway in TMZ-response on additional neurospheres from our repository. We estimated the expression correlations of MGMT – as a covariate for TMZ response – with the set of 11 Hh-pathway component genes on A49910, M45481, B0027, B0043, B0048 and B0051 neurospheres. As shown in Figure 5, MGMT expression correlated well with the expressions of GLI1 and SNAI1, in all the neurospheres only except in M45481. Unlike the other 5 neurospheres, expressions of GLI1/SNAI1 vs. MGMT were clearly discordant in this neurosphere. As shown in Figure 5 a, GLI1/SNAI1 expression in M45481 was as high as B0048 but MGMT expression was 61.3 fold lower than B0048. Therefore, we estimated expression correlation of the 11 Hh-pathway component genes with MGMT on the 5 neurospheres excluding M45481. For the rest of 5 neurospheres, A49910 and B0027 were responders whereas B0043, B0050 and



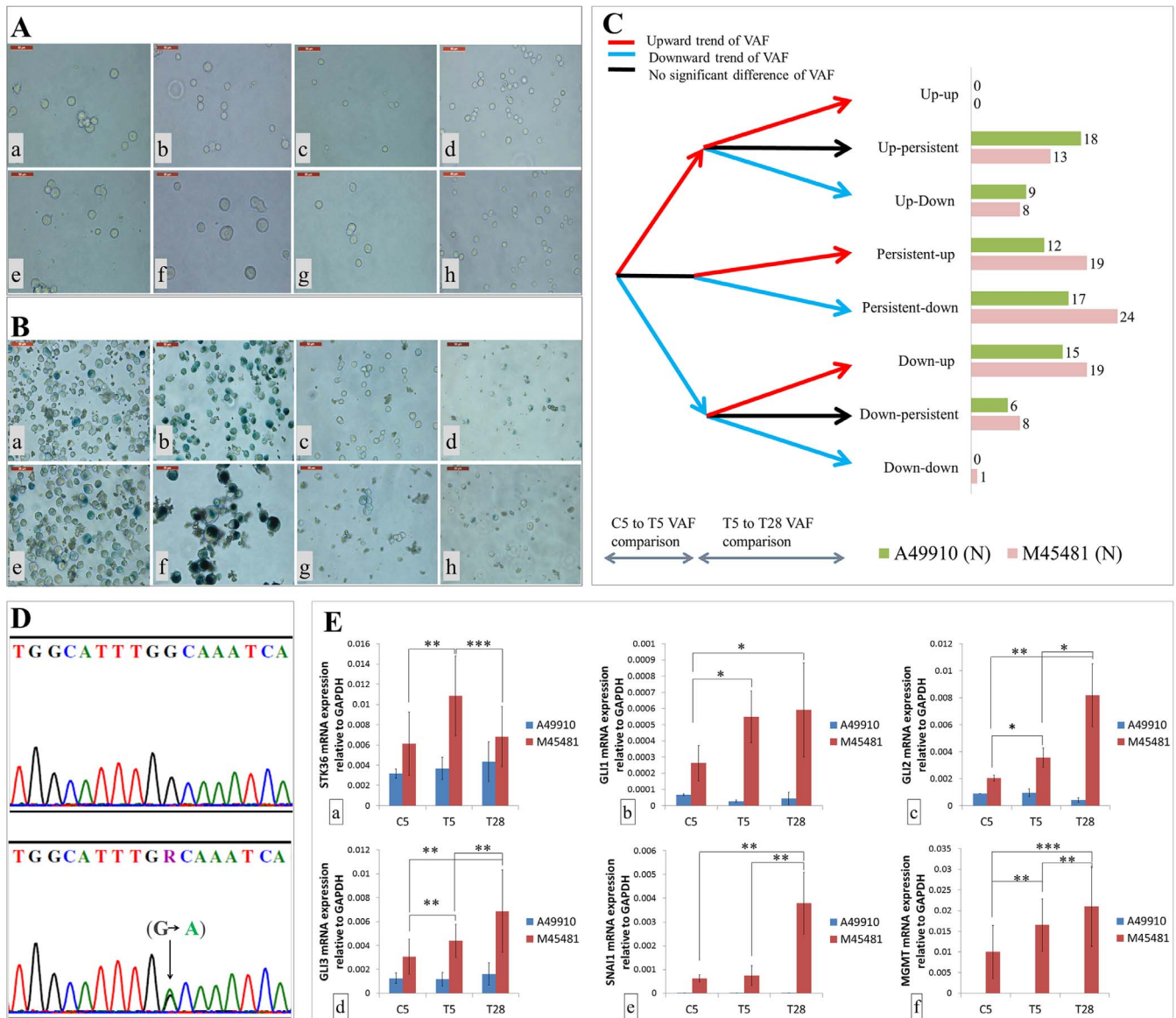


**Figure 4** | (A) Light microscopic images (50  $\mu$ m bar) at single cellular level. (a), day 5 DMSO-treated control cells of A49910, (b), day 28 DMSO-treated control cells of A49910. (c), day 5 DMSO-treated control cells of M45481, (d), day 28 DMSO-treated control cells of M45481, (e), day 5 TMZ-treated cells of A49910, (f), day 28 post-TMZ-treated cells of A49910, (g), day 5 TMZ-treated cells of M45481, and (h), day 28 post-TMZ-treated cells of M45481. (B) Light microscopic images (50  $\mu$ m bar) of the cells showing SA- $\beta$ -Gal staining following TMZ treatment and post-treatment recovery. (a), day 5 DMSO-treated control cells of A49910, (b), day 28 DMSO-treated control cells of A49910, (c), day 5 DMSO-treated control cells of M45481, (d), day 28 DMSO-treated control cells of M45481, (e), day 5 TMZ-treated cells of A49910, (f), day 28 post-TMZ-treated cells of A49910, (g), day 5 TMZ-treated cells of M45481, and (h), day 28 post-TMZ-treated cells of M45481. (C) VAFs showing biphasic trends where the first phase is the comparison of VAFs between C5 to T5 and second phase is the comparison of VAFs between T5 to T28. Red arrows are showing enriching VAFs in upward direction, blue showing downward direction and black showing no significant change. The green and purple horizontal bars on the right side represent the number of genes (N) in each category in A49910 and in M45481 respectively. (D) Sanger sequencing chromatogram showing a G to A transition on STK36 gene (arrow mark) in M45481 (lower panel) but not in A49910 (upper panel). (E) Showing mRNA expression patterns of Hh-pathway component genes, STK36 (a), GLI1 (b), GLI2 (c), GLI3 (d), Hh-pathway target gene SNAI1 (e) and MGMT (f) following TMZ-treatment and post-treatment recovery (C5, DMSO treated control; T5, day-5 TMZ-treated; T28, day-28 post-treatment recovery, \*p-value < 0.05, \*\*p-value < 0.01 and \*\*\*p-value < 0.001).

B0051 were non-responders as revealed by annexin V and CFSE staining experiments (data not shown). We found statistically significant correlations of expression of MGMT with that of the key component genes of the Hh-pathway GLI1 ( $r = 0.9939$ ), SNAI1 ( $r = 0.9917$ ) and SUFU ( $r = 0.964$ ); ( $|r| = 0.96$  is the 10% False Discovery Rate cutoff for significance). Linear regression of GLI1 on MGMT (Adjusted  $R^2 = 0.9839$ , p-value 0.00056) and that of SNAI1 on MGMT (Adjusted  $R^2 = 0.9752$ , p-value 0.008286), as in Figures 5 c and d respectively, suggest the Hh-pathway to be playing a significant role in TMZ-response of the GBM neurospheres.

**Validation on TCGA-GBM database as a large clinical cohort of GBM.** In order to further validate the correlations of expression of MGMT expression with that of GLI1 and SNAI1 on GBM patients, we downloaded TCGA-GBM RNA-Seq V2 database and extracted the whole transcriptomics data on 149 patients from the database<sup>17</sup>. mRNA expression of MGMT showed statistically significant correlation with that of SNAI1 (Spearman  $r = 0.2678$ , p-value 0.0010,  $N = 149$ ) but surprisingly did not show significant (p-value 0.09) correlation with GLI1 (as given in the Supplementary Figure S1).



**Table 1** | The selected list of genes where VAFs enriched above 70% and/or the genes significantly altered relevant pathways as revealed by IPA in A49910 and M45481.

Chromosome#	Locus	VAFs at C5	VAFs at T5	VAFs at T28	Hugo Symbol	Significantly altering pathways as detected by Ingenuity pathway analysis (IPA)
<b>A49910</b>						
11	8752598	72.73%	40%	94.74%	ST5	None
1	228494790	63.33%	50%	85.29%	OBSCN	None
1	11579470	30%	66.67%	78.79%	PTCHD2	None
7	91712698	70%	60%	77.50%	AKAP9	None
1	26883511	39.13%	37.50%	73.81%	RPS6KA1	Cell cycle G2/M DNA damage checkpoint regulation
10	37506700	50%	42.86%	72.22%	ANKRD30A	None
8	48798539	57.30%	35.82%	71.62%	PRKDC	Double strand break repair by non-homologous end joining
<b>M45481</b>						
13	39343807	52.38%	51.04%	76.54%	FREM2	None
17	56388238	68%	43.86%	73.33%	BZRAP1	None
6	116973182	60%	36.84%	70.83%	ZUFSP	None
4	57248716	35.44%	56.73%	42.37%	AASDH	Lysine II, V and phenylalanine degradation pathway
2	219557978	27.78%	16.54%	38.66%	STK36	Sonic hedgehog signalling pathway

**TMZ-sensitization of a TMZ-non-responder neurosphere *in vitro* by Hh-pathway inhibitor vismodegib.** However, in order to further understand the link between TMZ-response and the Hh-pathway in GBM we performed a proof of principle experiment *in vitro*. We performed this experiment on the most TMZ-resistant neurosphere (B0048) from our repository. As shown in Figure 6 a, b and the first two columns of e, there was no significant apoptosis induced by TMZ-treatment alone to this neurosphere *in vitro* (p-value 0.179). But a 3.2 fold increase (p-value 0.0004) in the total number of apoptotic cells in the same neurosphere was observed when the TMZ-treatment was done along with the FDA-approved Hh-pathway inhibitor drug vismodegib treatment *in vitro* (Fig. 6 e). Vismodegib treatment alone induced 2.2 fold (p-value 0.0011) apoptosis compared to the DMSO-treated control (Fig. 6 e). These results suggest the Hh-pathway could be a potential therapeutic target to enhance TMZ-response in this malignancy.

## Discussion

To summarize, we have three major components to our study. First, we describe a model that explains varied TMZ-response of GBM. We observed the response of heterogeneous pool of GBM neoplastic cells treated with the maximum clinically achievable dose of the DNA-damaging chemotherapeutic agent TMZ *in vitro*. We determined that the residual cells demonstrated either sustained growth arrest followed by cellular senescence (in responder patient-derived neurosphere) or a transient cell-cycle arrest followed by a reversible drug-effect (in non-responder patient-derived neurosphere). Such reversible cell-cycle arrest by TMZ-treatment in GBM neurospheres *in vitro* was previously reported by Mihaliak *et al.*<sup>14</sup>. Induction of cellular senescence is recognized as an indicator of good TMZ-response in GBM<sup>18</sup> but not much is known about the mechanisms. TMZ chemotherapy in patients is given in 28-day cycles – 5 days of treatment and 23 days of recovery<sup>1</sup>. The later period allows patients to recover from the toxic effects of the drug and prepare for the next cycle, as do the neoplastic cells unless the drug effect is sustained in them. If GBM neoplastic cells do indeed show a sustained TMZ-effect via the induction of TICS during the recovery period, this could have a profound impact on the final outcome of TMZ chemotherapy. Suggesting, the fate of residual clones, either a sustained response or a reversible drug-effect following TMZ treatment, could be very important.

The second component of our study was to identify the genetic basis of residual clones demonstrating either TICS or reversible growth-arrest. We explored the genetic heterogeneity of the neurospheres in order to identify the “specific set of mutations” that are

enriching in presence of TMZ *in vitro*. It is a long standing argument whether a resistant clone in a tumor is preexisting or generated *de-novo* by harsh treatment from a mutagenic or DNA damaging drug (such as TMZ). Regardless of origin, if a clone is altered upon TMZ exposure it will be reflected on the mutation spectrum by an enrichment of VAFs on loci throughout its genome. As we currently do not have a proper tool to address the dynamics of clonal heterogeneity, deep DNA sequencing technology is the only method which might be able to shed some light on this<sup>13</sup>. We used this method in TMZ-treated GBM neoplastic cells and found enrichment of VAFs on 45 genes in cells showing TICS (e.g., ST5, PRKDC and RPS6KA1) and on 51 genes in cells showing reversible TMZ-effect (e.g., FREM2, AASDH and STK36). These genes are relevant to the respective phenotypes observed in the two neurospheres. For instance, the A49910 neurosphere, which displayed flattened residual cell morphology, we found highest enrichment of VAF in the ST5 gene, which is involved in cytoskeletal reorganization<sup>19</sup>. Two genes enriched in the A49910 neurosphere following TMZ-treatment play central roles in the DNA damage response (DDR) pathways: PRKDC encodes for the catalytic subunit of the DNA-dependent protein kinase (DNA-PKCs), and RPS6KA1, encodes for a member of the RSK (ribosomal S6 kinase) family of serine/threonine kinases<sup>20–22</sup>. In the M45481 the highest enrichment of VAF was in FREM2, which encodes for an extracellular matrix component, associated with cellular migration and motility<sup>23</sup>. The M45481 also demonstrated lysine-II&V/phenylalanine degradation pathway via AASDH and sonic hedgehog (Hh) pathway via STK36<sup>24,25</sup>. The role of AASDH in cellular senescence/quiescence is not well defined, but amino acid degradation pathways in general can have significant impact on cell survival<sup>26</sup>. The Hh-pathway is a developmentally important signaling pathway known to be involved in proliferation, migration and survival of cancer cells<sup>15,27,28</sup>. All four signaling pathways detected by our analysis may be relevant to their respective phenotypes, but for the current study we selected the Hh-pathway for further validation experiments.

The third and last component of our study was validation. To begin, we confirmed the existence of the variant locus (G to A transition) on the STK36 gene by Sanger sequencing. The biological importance of this specific mutation on the STK36 gene is not yet clear to us at this moment. Serine/Threonine kinase STK36 alias “Fused (Fu)” is a key component of the Hh-pathway<sup>24,25</sup>. Experimentally knocking out this gene impairs the Hh-pathway activity but the kinase function of STK36 is not responsible for its key role in the Hh-pathway<sup>24</sup>. In a high throughput siRNA based functional assay<sup>29</sup>, silencing of STK36 gene sensitizes established cultured cells to DNA damaging agents (PARP inhibitors), thereby suggesting its role in DDR. We

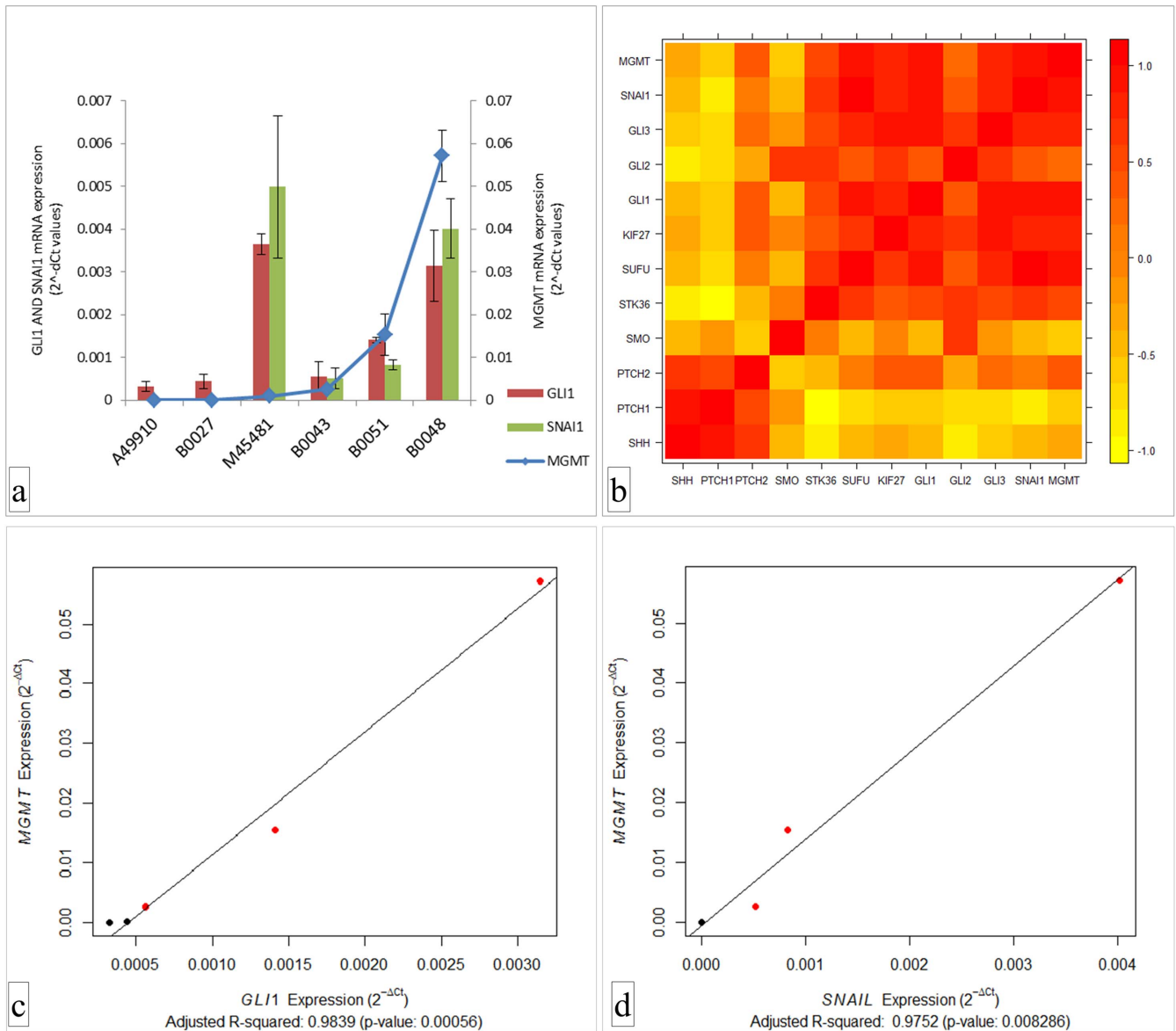


**Figure 5** | (a), mRNA expressions of GLI1, SNAI1 and MGMT in 6 neurospheres. (b), Correlation matrix of 11 Hh-pathway component genes and MGMT ( $|r| = 0.96$  FDR 0.1) on 5 cells except M45481. (c), Regression model fitting with the expressions of GLI1 with MGMT and (d), SNAI1 with MGMT. Red dots representing non-responder cells and black dots responder cells.

observed a statistically significant increase of the Hh-pathway activity in response to DNA-damaging insult by TMZ in M45481 cells but not in A49910 cells. This also suggests an important role for the Hh-pathway in DDR.

For further validation using additional GBM neurospheres in our repository we selected MGMT as a covariate of TMZ-response<sup>30,31</sup> in order to estimate its expression correlation with the 11 canonical Hh-pathway component genes. They correlated well excluding the neurosphere M45481, which showed discordance in terms of MGMT and GLI1/SNAI1 expression patterns. The relative levels of GLI1/SNAI1 expressions in this neurosphere were as high as that of the most TMZ-resistant neurosphere B0048 but MGMT expression was 61.3 fold lower than B0048. However, despite being 61.3 fold lower than B0048, MGMT expression in M45481 neurosphere appeared to be more than 200 fold higher than that of the responder neurosphere A49910. Phenotypically, the neurosphere M45481 initially responded to TMZ-treatment *in vitro* but reverted back within 3–4 weeks of drug withdrawal. Therefore, in spite of showing an initial response to TMZ-treatment this neurosphere finally behaved like a non-responder. This

“reversible non-response” phenotype was repeatedly observed in this neurosphere but we have no more such “reversible non-responder” neurospheres in our repository at this moment. Therefore, it could not be classified as a separate group and was excluded from this correlation analysis.

The patterns of MGMT expression in patient biopsy samples and in the neurospheres were tightly correlated. Interestingly, MGMT expression in the neurospheres of A49910, B0027 and M45481 was lower than in their corresponding tumor biopsies but it remained either unchanged in B0043 or even increased in B0048 and in B0051 neurospheres compared to their corresponding tumor biopsies. As further investigation was outside of our main area of study, we cautiously interpret these results as follows. Freshly resected tumor biopsy tissues can contain “non-tumor” cells, such as leukocytes, untransformed glial cells or even normal neurons. It is unlikely that MGMT is silenced in these normal cells, suggesting a relatively higher MGMT expression in biopsies (which is mixed up with normal cells) compared to the corresponding responder neurospheres. On the other hand, MGMT could be overexpressed in non-responder neurospheres

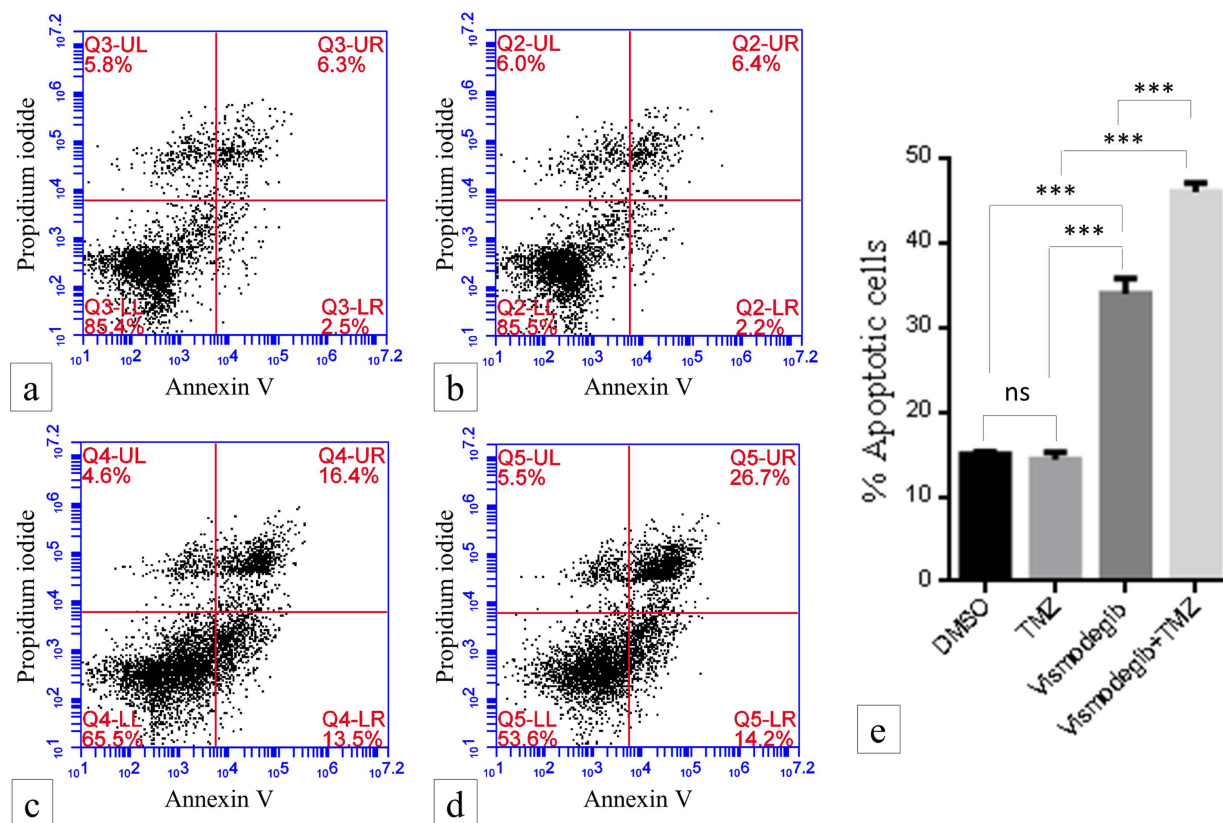


**Figure 6** | Flow cytometry analysis of annexin-V and propidium iodide (PI) staining of apoptotic cells following vismodegib (50  $\mu$ M) and TMZ (50  $\mu$ M) treatment to B0048 neurosphere. a), DMSO-treated control, b), TMZ treatment alone, c) vismodegib treatment alone, d), TMZ treatment along with vismodegib treatment and e), showing % of apoptotic cells (annexin-V positive + PI positive + annexin-V and PI double positive cells). (\* p-value < 0.05, \*\* p-value < 0.01 and \*\*\* p-value < 0.001).

compared to the normal cells. Therefore the resultant MGMT expression could be higher in the non-responder neurospheres compared to their corresponding tumor biopsies.

In our results MGMT expression was correlated with the expressions of GLI1 and SNAI1, as well as with direct TMZ-response of these neurospheres *in vitro*. Although it is not a direct measure, MGMT expression is the closest measure of TMZ-response in GBM. Therefore we further tested the correlation of expression of MGMT with that of GLI1 and SNAI1 in the TCGA-GBM database with partial validation. MGMT expression was significantly correlated with SNAI1 but poorly correlated with GLI1. This indicates the possible influence of Hh-pathway intermediate factor (s) or co-factor (s) in GBM *in vivo* which could be a subject of further investigation. Finally, as a proof of principle experiment *in vitro* we demonstrated TMZ-sensitization of a TMZ-resistant neurosphere by treatment with the FDA approved pharmacological Hh-pathway inhibitor vismodegib. That is encouraging from the translational point of view and subject to a separate investigation including more *in vitro* experiments and preclinical mouse models.

The role of the Hh-pathway is known in various aspects of cancer cell biology but its role in chemoresistance is unclear. Recently, mechanistic details of how Hh-transcription factor GLI1 and SNAI1 impart chemoresistance in Acute Myeloid Leukemia (AML) have been explained<sup>32</sup>. Moreover, inhibition of the Hh-pathway together with the PI3K pathway is a better therapeutic option than inhibition of PI3K alone<sup>33</sup>. Precise mechanistic details of how Hh-pathway confers TMZ chemoresistance in GBM are currently being explored in our laboratory. In the present paper we demonstrated an *in vitro* model of clonal enrichment analysis by exome wide enrichment of VAFs in response to TMZ-treatment and post-treatment recovery. The TMZ-treatment and post-recovery model *in vitro* was shown before by

Mihaliak *et al.*<sup>14</sup> and we have utilized this model to further understand the genetic basis of the residual clones showing sustained versus reversible TMZ-effect. To our understanding this is a first study of this kind where genetic heterogeneity of GBM neurospheres in response to TMZ *in vitro* has been explored as a discovery scale experiment to find out the genes and pathways responsible for TMZ-response. With this analysis we found the Hh-pathway to hinder sustained TMZ-response in GBM neoplastic cells. Therefore, there is a strong possibility of induction of apoptosis/cellular senescence in GBM neoplastic cells if the Hh-pathway is kept suppressed while treating GBM with TMZ. Clinically, inhibition of this pathway could be a potential strategy to enhance sustained TMZ-response in this malignancy.

## Methods

**Patient follow-up in clinic.** Following the guidelines of the Declaration of Helsinki, all patients provided written consent in compliance with institutional review board (IRB) approvals from their respective institutes and hospitals. All methods were carried out in accordance with the NIBMG, India, Ethical Committee approved guidelines. Details of the patients' clinical follow-up information are given in the Supplementary Information.

**Collection of tumor tissues and isolation of neurospheres.** Fresh tumor tissues were collected from Operation Theater immediately after surgery. We utilized approximately 0.2 to 0.5 centimeter (~ size of a pencil eraser) sizes of resected tumors from patients to make single cell suspensions in order to develop neurospheres. Single-cell suspensions from tumor tissues were made by enzymatic digestion with Liberase selection grade (Roche Diagnostics GmbH, Germany, cat# 114106). The suspensions were treated with RBC lysis buffer for 5 minutes at room temperature. Then the suspensions were washed two times with ice cold PBS (1X) and finally the cell pellets were re-suspended and seeded with StemPro<sup>®</sup> NSC SFM media (Invitrogen, NY, USA cat# A10509-01) at standard mammalian tissue culture conditions to grow them as neurospheres. Approximately 4–5 million viable cells (as counted by trypan blue exclusion test at the final step) were seeded in 4ml of media in



a T-25 flask for developing neurospheres. We isolated 6 neurospheres A49910, M45481, B0027, B0043, B0048 and B0051 for our current study.

**TMZ treatment to the neurospheres *in vitro*.** Patient-derived neurospheres were treated with either 50  $\mu\text{M}$  TMZ (Sigma-Aldrich, MO, USA cat# 76899) or with 0.1% DMSO (as vehicle control) for 5 days. Then the drug was withdrawn and the neurospheres were further grown for 23 days without drug. At the end of 5 days and 28 days they were trypsinized into single-cell suspensions and viable cell numbers were determined by hemocytometer following a standard trypan blue exclusion test. All images of the neurospheres and single cells were documented with inverted microscope Leica DM IL LED using the software Leica Application Suite Version 3.7.0 (Leica Microsystems GmbH, Germany).

**Growth curve analysis of neurospheres by MTS assay.** Growth curve was determined by standard MTS assay using CellTiter 96<sup>R</sup> Aqueous One Solution Cell Proliferation Assay System (Promega Corporation, WI, USA cat# G3580) following manufacturer's protocol. MTS assay was done in triplicates at 4 different time points (0<sup>th</sup>, 1<sup>st</sup>, 3<sup>rd</sup> and 5<sup>th</sup> day) after 5 days of treatment and 28 days of post-treatment recovery.

**Tracking cell division for 28 days by CFSE staining.** Single cell suspensions of neurospheres were stained with Carboxyfluorescein succinimidyl ester (CFSE) using CellTrace™ CFSE Cell Proliferation Kit (Life technologies, Oregon, USA cat# C34554) following manufacturer's protocol. The stained cells were divided into two equal parts, one part treated with DMSO and the other part was treated with 50  $\mu\text{M}$  TMZ for 5 days. CFSE staining intensities were measured by flow cytometry (BD Acuri™ C6, BD BioSciences, USA) after 5 days of treatment and at 28 days of post-treatment recovery.

**Senescence associated  $\beta$ -Gal (SA- $\beta$ -Gal) staining.** SA- $\beta$ -gal staining was done to determine cellular senescence using cellular senescence assay kit (Chemicon International, MA, USA cat # KAA002) following manufacturer's protocol. Briefly, approximately  $5 \times 10^5$  cells were washed with 1x PBS, fixed by fixing solution provided with the kit, stained overnight with 2 ml freshly prepared 1x SA- $\beta$ -gal detection solution and observed under phase contrast microscopy.

**DNA/RNA extraction and quantitative reverse transcriptase polymerase chain reaction (qRT-PCR) analysis.** All DNA and RNA were extracted from cells using AllPrep DNA/RNA Mini Kit (Qiagen GmbH, Germany cat# 80204). Reverse transcription was done using High Capacity cDNA Reverse Transcription Kit (Applied Biosystems, UK cat# 4368814) Quantitative measurements of target gene expression relative to either  $\beta$ -Actin or 18s RNA or GAPDH were performed in triplicates using Power SYBR Green PCR Master Mix (Applied Biosystems, UK cat# 4368706) following the manufacturer's recommendations in an ABI 7900HT Fast Real Time PCR system. Relative expression was defined by  $2^{-\Delta\Delta Ct}$  method<sup>34</sup>. Error bars were generated from the triplicate  $^{-\Delta Ct}$  values. The primer sequences are given in the Supplementary Table S18.

**Whole exome sequencing (WES) experiments.** Libraries for WES were constructed and sequenced on an Illumina HiSeq2000 using 100 bp paired-end reads following manufacturer's guidelines. Image analysis and base calling were performed using the Illumina Real Time Analysis (RTA) Pipeline version 1.12 with default parameters as previously reported<sup>35</sup>. Details of the experiments are given in Supplementary Information.

**Analysis of variant allele frequency (VAF).** VAF at a locus was defined as the proportion of the variant allele observed by the total depth at that position. Difference in VAF was measured using standardized two-sample Z Statistic. If  $p_1$  be the VAF at a locus at time  $t_1$  ( $t_1$  can be Day5 control (C5), Day5 TMZ-treated (T5) and Day 28 post-treatment recovery (T28)) with depth  $n_1$  and  $p_2$  be the VAF for the same locus at a different time point  $t_2$  ( $t_2$  can be C5, T5 and T28 but not  $t_1$ ) with depth  $n_2$ , the standardized Z Statistic with asymptotically normal properties is defined as

$$Z = \frac{p_1 - p_2}{\sqrt{(p(1-p)) \left[ \frac{1}{n_1} - \frac{1}{n_2} \right]}} \text{ where, } p = (n_1 p_2 + n_2 p_1) / (n_1 + n_2).$$

We ranked all the significantly different VAFs based on their  $Z^2$  values and preselected the top 1% in order to reduce false positive results.

**Bioinformatic analyses of significantly altered pathways.** Significantly over-represented pathways were identified using Ingenuity Pathway Analysis (IPA) web based application (accessed on 1<sup>st</sup> Aug, 2013). We downloaded the RNA-Seq based whole transcriptomics data available as open access (<https://tcga-data.nci.nih.gov/tcga/> accessed on May 20<sup>th</sup> 2014) and extracted gene expression results of the already published TCGA-GBM clinical cohort<sup>17</sup>.

**TMZ-sensitization of a TMZ non-responder neurosphere by inhibition of Hh-pathway *in vitro*.** For this experiment we preselected a non-responder neurosphere from our repository (B0048) which was the most resistant to TMZ-treatment *in vitro*. We treated the cells either with maximum clinically achievable dose (50  $\mu\text{M}$ ) of vismodegib (Selleckchem, Houston, TX, USA, cat # S1082) or DMSO (0.1%) as

placebo consecutively for 5 days. After 5 days both the DMSO-treated cells and vismodegib-treated cells were sub-divided into two parts. One part was treated with TMZ (50  $\mu\text{M}$ ) and the other part was continued with DMSO treatment. Similarly, the one part of the vismodegib-treated cells was treated with TMZ (50  $\mu\text{M}$ ) along with vismodegib (50  $\mu\text{M}$ ) and the other part was continued with vismodegib treatment alone. Annexin-V and propidium iodide staining was done on the cells after this complete course of treatment (altogether for 10 days). The number of apoptotic cells in each treatment was detected by flow cytometry analysis (BD Acuri™ C6, BD BioSciences, USA). The data presented as the total number of apoptotic cells in each treatment. The whole experiment was done in triplicate and the error bars were calculated from the independently repeated experiments.

**Statistical analyses.** To compare the differences in viable cell numbers of DMSO- and TMZ- treated cells, for the  $i^{\text{th}}$  set of experiments, we translated the number of viable TMZ-treated cells as percentage of viable DMSO-treated cells ( $u_i$ ). The mean of  $u_i$  was compared with 100, using univariate t-test. Student's t-test was used to compare the gene expressions by quantitative RT-PCR experiments. We fitted a linear regression to approximate the growth curve by MTS assays. Days were taken as the independent variable (0, 1, 3, and 5) and OD values of MTS assays as dependent variable. For each cell two separate regressions were fitted using the control and the TMZ treated OD values. The slope of these two regression equations were compared both in day 5 and in day 28. Pearson's correlation coefficients ( $r$ ) were determined on the expression of 11 canonical Hh-pathway component genes and MGMT in the neurospheres. Multiple testing correction was done with a False Discovery Rate<sup>36</sup> of 10%, to find out significant correlations. All statistical analyses were done using R 3.1 (<http://www.r-project.org>) and GraphPad Prism 6 (<http://www.graphpad.com>).

- Stupp, R. *et al.* Radiotherapy plus concomitant and adjuvant temozolomide for glioblastoma. *The New England journal of medicine*. **352**, 987–996 (2005).
- Hoeijmakers, J. H. DNA damage, aging, and cancer. *The New England journal of medicine* **361**, 1475–1485 (2009).
- Denny, B. J., Wheelhouse, R. T., Stevens, M. F., Tsang, L. L. & Slack, J. A. NMR and molecular modeling investigation of the mechanism of activation of the antitumor drug temozolomide and its interaction with DNA. *Biochemistry*. **33**, 9045–9051 (1994).
- Roos, W. P. & Kaina, B. DNA damage-induced cell death by apoptosis. *Trends in molecular medicine* **12**, 440–450 (2006).
- Ciccia, A. & Elledge, S. J. The DNA damage response: making it safe to play with knives. *Molecular cell*. **40**, 179–204 (2010).
- Shpitsin, M. *et al.* Molecular definition of breast tumor heterogeneity. *Cancer cell*. **11**, 259–273 (2007).
- Brock, A., Chang, H. & Huang, S. Non-genetic heterogeneity--a mutation-independent driving force for the somatic evolution of tumours. *Nat Rev Genet*. **10**, 336–342 (2009).
- Marusyk, A., Almendro, V. & Polyak, K. Intra-tumour heterogeneity: a looking glass for cancer? *Nature reviews*. **12**, 323–334 (2012).
- Almendro, V., Marusyk, A. & Polyak, K. Cellular heterogeneity and molecular evolution in cancer. *Annual review of pathology*. **8**, 277–302 (2013).
- Patel, A. P. *et al.* Single-cell RNA-seq highlights intratumoral heterogeneity in primary glioblastoma. *Science (New York, N.Y.)*. **344**, 1396–1401 (2014).
- Newlands, E. S. *et al.* Phase I trial of temozolomide (CCRG 81045: M&B 39831: NSC 362856). *British journal of cancer*. **65**, 287–291 (1992).
- Shackleton, M., Quintana, E., Fearon, E. R. & Morrison, S. J. Heterogeneity in cancer: cancer stem cells versus clonal evolution. *Cell*. **138**, 822–829 (2009).
- Aparicio, S. & Caldas, C. The implications of clonal genome evolution for cancer medicine. *The New England journal of medicine*. **368**, 842–851 (2013).
- Mihaliak, A. M. *et al.* Clinically relevant doses of chemotherapy agents reversibly block formation of glioblastoma neurospheres. *Cancer letters*. **296**, 168–177 (2010).
- Amakye, D., Jagani, Z. & Dorsch, M. Unraveling the therapeutic potential of the Hedgehog pathway in cancer. *Nature medicine*. **19**, 1410–1422 (2013).
- Axelson, M. *et al.* U.S. Food and Drug Administration approval: vismodegib for recurrent, locally advanced, or metastatic basal cell carcinoma. *Clin Cancer Res*. **19**, 2289–2293 (2013).
- Brennan, C. W. *et al.* The somatic genomic landscape of glioblastoma. *Cell*. **155**, 462–477 (2013).
- Chitikova, Z. V. *et al.* Sustained activation of DNA damage response in irradiated apoptosis-resistant cells induces reversible senescence associated with mTOR downregulation and expression of stem cell markers. *Cell cycle (Georgetown, Tex)*. **13**, 1424–1439 (2014).
- Hubbs, A. E., Majidi, M. & Lichy, J. H. Expression of an isoform of the novel signal transduction protein ST5 is linked to cell morphology. *Oncogene*. **18**, 2519–2525 (1999).
- Roukos, V. *et al.* Spatial dynamics of chromosome translocations in living cells. *Science (New York, N.Y.)*. **341**, 660–664 (2013).
- Novotna, E. *et al.* DNA-dependent protein kinase and its inhibition in support of radiotherapy. *International journal of radiation biology*. **89**, 416–423 (2013).
- Houslay, M. D. A RSK( $\gamma$ ) relationship with promiscuous PKA. *Sci STKE*. **2006**, pe32 (2006).
- Timmer, J. R., Mak, T. W., Manova, K., Anderson, K. V. & Niswander, L. Tissue morphogenesis and vascular stability require the Frem2 protein, product of the



- mouse myelencephalic blebs gene. *Proceedings of the National Academy of Sciences of the United States of America*. **102**, 11746–11750 (2005).
24. Murone, M. *et al.* Gli regulation by the opposing activities of fused and suppressor of fused. *Nature cell biology*. **2**, 310–312 (2000).
  25. Wilson, C. W. *et al.* Fused has evolved divergent roles in vertebrate Hedgehog signalling and motile ciliogenesis. *Nature*. **459**, 98–102 (2009).
  26. Struys, E. A. & Jakobs, C. Metabolism of lysine in alpha-aminoadipic semialdehyde dehydrogenase-deficient fibroblasts: evidence for an alternative pathway of pipercolic acid formation. *FEBS letters*. **584**, 181–186 (2010).
  27. Feldmann, G. *et al.* Blockade of hedgehog signaling inhibits pancreatic cancer invasion and metastases: a new paradigm for combination therapy in solid cancers. *Cancer research*. **67**, 2187–2196 (2007).
  28. Karhadkar, S. S. *et al.* Hedgehog signalling in prostate regeneration, neoplasia and metastasis. *Nature*. **431**, 707–712 (2004).
  29. Turner, N. C. *et al.* A synthetic lethal siRNA screen identifying genes mediating sensitivity to a PARP inhibitor. *The EMBO journal*. **27**, 1368–1377 (2008).
  30. Hegi, M. E. *et al.* MGMT gene silencing and benefit from temozolomide in glioblastoma. *The New England journal of medicine*. **352**, 997–1003 (2005).
  31. Butowski, N. *et al.* Phase II and pharmacogenomics study of enzastaurin plus temozolomide during and following radiation therapy in patients with newly diagnosed glioblastoma multiforme and gliosarcoma. *Neuro-oncology*. **13**, 1331–1338 (2011).
  32. Zahreddine, H. A. *et al.* The sonic hedgehog factor GLI1 imparts drug resistance through inducible glucuronidation. *Nature*. **511**, 90–93 (2014).
  33. Gruber Filbin, M. *et al.* Coordinate activation of Shh and PI3K signaling in PTEN-deficient glioblastoma: new therapeutic opportunities. *Nature medicine*. **19**, 1518–1523 (2013).
  34. Pfaffl, M. W. A new mathematical model for relative quantification in real-time RT-PCR. *Nucleic acids research*. **29**, e45 (2001).
  35. Maitra, A. *et al.* Mutational landscape of gingivo-buccal oral squamous cell carcinoma reveals new recurrently-mutated genes and molecular subgroups. *Nature communications*. **4**, 2873 (2013).
  36. Benjamini, Y. H. Yosef Controlling the false discovery rate: a practical and powerful approach to multiple testing. *Journal of the Royal Statistical Society*. **57**, 289–300 (1995).

## Acknowledgments

We thank all the patients and patient families for their kind cooperation and constant support. We are thankful to Dr. Gregory Riggins at the Johns Hopkins University School of Medicine, Baltimore, MD, USA for his valuable suggestions while developing the neurospheres in our laboratory. We are especially grateful to Dr. Carrie L. Iwema, University of Pittsburgh, PA, USA for carefully reviewing this manuscript. We acknowledge Dr. Samsiddhi Bhattacharjee, NIBMG, India, for the fruitful discussions in developing statistical methods. We thank Biswanath Bhattacharya, NIBMG, Sarita Misra, AMRI

hospitals, and Subhro Majumder, Medica Superspecialty Hospital, for helping with patient records and following up patients in clinic. We acknowledge Prof. Sharmila Sengupta and Ms. Paramita Mandal, NIBMG, for helping us with IHC experiments, Dr. Sandeep Singh, NIBMG for helping us with flow cytometry experiments. We acknowledge the members of NIBMG DNA sequencing and Microarray laboratories. We thank Prof. Partha P. Majumder, Director, NIBMG, for all the fruitful academic discussions and also for supporting us with institutional funds.

## Author contributions

The senior (last) author S.D. conceived the idea, designed the study, performed the lead experiments to develop the model system in the laboratory and wrote the manuscript with inputs from other authors. V.C. performed the *in vitro* experiments of annexin V, CFSE and qRT-PCR; N.K.B. developed the pipeline of analysis of NGS data along with A.M., S.K. and S.D. (co-first authors N.K.B. and V.C. equally contributed to the work). N.S.R. performed the SNP-Chip microarray experiments and analysed the data; R.N.B., L.N.T. and S.K.B. performed the intracranial surgeries and helped with the clinical data; T.D. did the Immunofluorescence staining experiments; T.D. along with A.C. and P.B. did the experiments with MGMT; A.M. led the NGS library preparation and sequencing experiments; A.B. and A.M. helped with all the statistical analyses and with the design of the NGS analyses; A.C. helped with IPA. All authors have critically reviewed and approved the final manuscript in the present form.

## Additional information

**Accession number for data submission to European Nucleotide Archive (ENA):** Study accession number is PRJEB4923. Secondary study accession number is: ERP004260. Study unique name is: ena-STUDY-NIBMG-06-11-2013-06:41:03:355-125. The URL to study accession is <http://www.ebi.ac.uk/ena/data/view/PRJEB4923>

**Supplementary information** accompanies this paper at <http://www.nature.com/scientificreports>

**Competing financial interests:** The authors declare no competing financial interests.

This work was carried out by an intramural funding support from NIBMG, India.

**How to cite this article:** Biswas, N.K. *et al.* Variant allele frequency enrichment analysis *in vitro* reveals sonic hedgehog pathway to impede sustained temozolomide response in GBM. *Sci. Rep.* **5**, 7915; DOI:10.1038/srep07915 (2015).



This work is licensed under a Creative Commons Attribution-NonCommercial-NoDerivs 4.0 International License. The images or other third party material in this article are included in the article's Creative Commons license, unless indicated otherwise in the credit line; if the material is not included under the Creative Commons license, users will need to obtain permission from the license holder in order to reproduce the material. To view a copy of this license, visit <http://creativecommons.org/licenses/by-nc-nd/4.0/>

RESEARCH ARTICLE

# Hedgehog Signaling Pathway Is Active in GBM with GLI1 mRNA Expression Showing a Single Continuous Distribution Rather than Discrete High/Low Clusters

Vikas Chandra<sup>1</sup>✉, Tapojyoti Das<sup>1</sup>✉, Puneet Gulati<sup>2</sup>✉, Nidhan K. Biswas<sup>1</sup>, Sarang Rote<sup>2</sup>, Uttara Chatterjee<sup>3</sup>, Samarendra N. Ghosh<sup>2</sup>, Sumit Deb<sup>2</sup>, Suniti K. Saha<sup>4</sup>, Anup K. Chowdhury<sup>2</sup>, Subhashish Ghosh<sup>2</sup>, Charles M. Rudin<sup>5</sup>, Ankur Mukherjee<sup>1</sup>, Analabha Basu<sup>1</sup>, Surajit Dhara<sup>1</sup>\*

**1** National Institute of Biomedical Genomics, P.O. N.S.S. Kalyani, West Bengal 741251, India, **2** Bangur Institute of Neurology, 52/1A, S.N. Pandit Street, Bhawanipore, Kolkata 700098, India, **3** Institute of Post Graduate Medical Education and Research, 244 AJC Bose Road, Kolkata-700020, India, **4** Nil Ratan Sarkar Medical College and Hospital, 138, AJC Bose Road, Kolkata-700014, India, **5** Memorial Sloan-Kettering Cancer Center, 1275 York Avenue, New York, New York 10065, United States of America

✉ These authors contributed equally to this work.

\* Current address: Weill Cornell Graduate School of Medical Sciences of the Cornell University, Sloan-Kettering Division, New York, New York, United States of America

\* [sd1@nibmg.ac.in](mailto:sd1@nibmg.ac.in)



**OPEN ACCESS**

**Citation:** Chandra V, Das T, Gulati P, Biswas NK, Rote S, Chatterjee U, et al. (2015) Hedgehog Signaling Pathway Is Active in GBM with GLI1 mRNA Expression Showing a Single Continuous Distribution Rather than Discrete High/Low Clusters. PLoS ONE 10(3): e0116390. doi:10.1371/journal.pone.0116390

**Academic Editor:** Javier S Castresana, University of Navarra, SPAIN

**Received:** November 5, 2014

**Accepted:** December 8, 2014

**Published:** March 16, 2015

**Copyright:** © 2015 Chandra et al. This is an open access article distributed under the terms of the [Creative Commons Attribution License](https://creativecommons.org/licenses/by/4.0/), which permits unrestricted use, distribution, and reproduction in any medium, provided the original author and source are credited.

**Data Availability Statement:** All relevant data are within the paper and its Supporting Information files.

**Funding:** The authors received no specific funding for this work. This work was supported by an intramural fund of National Institute of Biomedical Genomics (NIBMG), India.

**Competing Interests:** The authors have declared that no competing interests exist.

## Abstract

Hedgehog (Hh) signaling pathway is a valid therapeutic target in a wide range of malignancies. We focus here on glioblastoma multiforme (GBM), a lethal malignancy of the central nervous system (CNS). By analyzing RNA-sequencing based transcriptomics data on 149 clinical cases of TCGA-GBM database we show here a strong correlation ( $r = 0.7$ ) between GLI1 and PTCH1 mRNA expression—as a hallmark of the canonical Hh-pathway activity in this malignancy. GLI1 mRNA expression varied in 3 orders of magnitude among the GBM patients of the same cohort showing a single continuous distribution—unlike the discrete high/low-GLI1 mRNA expressing clusters of medulloblastoma (MB). When compared with MB as a reference, the median GLI1 mRNA expression in GBM appeared 14.8 fold lower than that of the “high-Hh” cluster of MB but 5.6 fold higher than that of the “low-Hh” cluster of MB. Next, we demonstrated statistically significant up- and down-regulation of GLI1 mRNA expressions in GBM patient-derived low-passage neurospheres *in vitro* by sonic hedgehog ligand-enriched conditioned media (shh-CM) and by Hh-inhibitor drug vismodegib respectively. We also showed clinically achievable dose (50  $\mu$ M) of vismodegib alone to be sufficient to induce apoptosis and cell cycle arrest in these low-passage GBM neurospheres *in vitro*. Vismodegib showed an effect on the neurospheres, both by down-regulating GLI1 mRNA expression and by inducing apoptosis/cell cycle arrest, irrespective of their relative endogenous levels of GLI1 mRNA expression. We conclude from our study that this single continuous distribution pattern of GLI1 mRNA expression technically puts almost all GBM patients in a single group rather than discrete high- or low-clusters in terms of Hh-pathway

activity. That is suggestive of therapies with Hh-pathway inhibitor drugs in this malignancy without a need for further stratification of patients on the basis of relative levels of Hh-pathway activity among them.

## Introduction

Hedgehog (Hh) signaling pathway is a developmentally important signaling pathway[1], inactive in normal adult mature cells and found to be aberrantly hyper-activated in a wide range of malignancies [2–5]. Aberrant hyper-activation of this pathway was first identified in Gorlin's syndrome [6, 7], where an autosomal dominant mutation in the tumor suppressor gene PTCH1 predisposed patients to basal cell carcinoma (BCC) and/or central nervous system (CNS) malignancy medulloblastoma (MB) [8]. PTCH1 is a 12-pass transmembrane (TM) receptor which in absence of its ligand inhibits the other 7-pass TM receptor SMO, keeping it from transmitting the signal. When PTCH1 binds to the soluble ligand sonic hedgehog (SHH)—or inactivated by loss-of-function mutation, as in Gorlin's syndrome—this inhibition on SMO is withdrawn and the pathway is turned on. PTCH1 has 57% sequence homology and also functional similarity with another TM receptor PTCH2 [9, 10]. The major intracellular players of this pathway in human are STK36, a serine/threonine kinase also known as fused (Fu), suppressor of Fu (SuFu), KIF27, a member of mammalian kinesin family, and finally the signal is transduced by Hh-transcription factors GLI1, GLI2 and GLI3 [11]. GLI1 is the primary representative of the active Hh-pathway. GLI1 and/or GLI2 are up-regulated upon activation of this pathway and further regulate transcriptions of various target genes—for instance, SNAI1 is a bona fide target of GLI1 transcription factor [12]. Role of GLI3 is context dependent, shown to play opposing inhibitory roles [13].

Hh-pathway is aberrantly hyper-activated in 100% of BCC patients [14] and in approximately 30% of MB patients, mostly driven by a loss-of-function mutation in PTCH1[15]. Other than these two, Hh-pathway is ligand-driven in almost all other malignancies studied till date[4]. Ligand-driven Hh-pathway activity is more complex to understand—this activation could be through autocrine and/or paracrine mechanisms [16]. More than 50 registered clinical trials on various cancers are currently going on (<https://clinicaltrials.gov>, accessed on June 1<sup>st</sup> 2014) with a series of pharmacological Hh-pathway inhibitors [17]. Systemic administration of Hh-pathway inhibitor Vismodegib (GDC 0449) is already approved by the US Food and Drug Administration (FDA) for the clinical use in BCC[18]. Clinical trial results with MB is also satisfactory [2] [18, 19] but there have been disappointing results in ovarian and colon cancers—malignancies where the pathway is ligand-driven [20, 21]. More detailed investigations are needed to understand the relevance of this pathway in this class of malignancies.

Our disease model here is glioblastoma multiforme (GBM)—a lethal CNS malignancy showing dismal prognosis with standard clinical care of surgery, adjuvant radiotherapy and chemotherapy [22]. Pharmacological inhibition of ligand-driven, aberrantly hyper-activated Hh-pathway is a potential therapeutic approach in this malignancy[3]. Unlike MB, role of this pathway in GBM is less clearly understood. Moreover, some controversies have been raised about the relevance of this pathway in GBM. Dahmane *et al.*, in 2001 implicated importance of this pathway in brain development and in CNS tumorigenesis [23]. While Hu *et al.*, in 2003 presented evidence of lack of Hh pathway activity in high grade gliomas [24]. However, Bar *et al.*, in 2007 showed higher expression of GLI1 in 5 out of 19 GBM cases (26%) and found



good correlation with SHH ligand expression in these samples suggesting ligand-driven activity of Hh-pathway [25]. Very recently in 2013, Filbin *et al.*, demonstrated synergistic inhibition of PI3K— and Hh—pathway together as a better therapeutic approach in GBM [26]. We analyzed 11 canonical Hh-pathway component genes from the recently published [27] RNA sequencing (RNA-Seq) transcriptomics data on a large clinical sub-cohort (N = 149) of TCGA-GBM database (<https://tcga-data.nci.nih.gov/tcga/>, accessed on May 20<sup>th</sup> 2014). We compared Hh-transcription factor GLI1 mRNA expression of GBM with that of MB in order to have a better understanding of the comparative status of Hh-pathway activity in GBM relative to MB as a reference. We demonstrate here ligand-driven up-regulation and vismodegib-driven down-regulation of Hh-pathway activity and induction of apoptosis/cell-cycle arrest with clinically achievable dose of vismodegib to GBM patient-derived neurospheres *in vitro*.

## Materials and Methods

### Patient cohort and collection of tumor biopsy samples

The two ethical committees, institutional review board (IRB) of Bangur Institute of Neurology (BIN) and Review Committee for Protection of Research Risks to Humans (RCPRRH) of National Institute of Biomedical Genomics (NIBMG), both approved this study. Following the guidelines of the Declaration of Helsinki, written consents from all the patients (N = 19) were taken to include them in the study in compliance with IRB approvals of the respective institutes and hospitals. The patient diagnosis were confirmed by radiographic imaging (MRI/CT scan) followed by histopathology as the list of patients is given in the [S1 Table](#). Henceforth, our GBM cohort will be written as NIBMG-GBM. We used GLI1 gene expression data from the MB cases (N = 56) that were already published in NEJM 2009[19] along with a single case of MB from our repository. Also, we downloaded the RNA-Seq based whole transcriptomics data (<https://tcga-data.nci.nih.gov/tcga/> accessed on May 20<sup>th</sup> 2014) and extracted gene expression results of 11 canonical Hh-pathway component genes from the already published large sub-cohort (N = 149) of TCGA-GBM cases [27].

### Neurospheres culture *in vitro*

Single-cell suspensions were prepared from the tumor biopsy samples with the help of enzymatic digestion by Liberase selection grade (Roche Diagnostics GmbH, Mannheim, Germany, cat # 05401046001). Then they were seeded with StemPro NSC SFM media (Invitrogen, Grand Island, NY, USA cat # A10509-01) in tissue culture flasks and incubated for approximately two weeks at 37°C in a humidified chamber with 5% CO<sub>2</sub> till the appearance of neurospheres.

### Preparation of Shh-enriched conditioned media (Shh-CM)

HEK293-ShhNp cells (a kind gift from Philip Beachy's laboratory), were grown to ~ 80% confluency; growth medium was replaced with fresh StemPro NSC SFM medium and incubated for 48 hours. Active ligand Shh-enriched conditioned medium (Shh-CM) was then collected, filtered (pore size, 0.22 μm) and stored at -80°C in small aliquots.

### Shh-CM and vismodegib treatment to neurospheres *in vitro*

Vismodegib (GDC-0449) was purchased from Selleckchem LLC, USA (Cat# S1082) through Pro Lab Marketing Pvt. Ltd., India. Approximately 10<sup>6</sup> cells/ml/well from the single cell suspensions of GBM neurospheres were seeded in 6-well plates and treated with Shh-CM (50% v/v

with growth media) and clinically relevant doses (0 $\mu$ M, 25 $\mu$ M, 50 $\mu$ M and 100 $\mu$ M) of vismodegib for 5 days.

### DNA/RNA extraction and quantitative reverse transcriptase polymerase chain reaction (qRT-PCR)

DNA/RNA was extracted using AllPrep DNA/RNA mini kit (Qiagen GmbH, Germany cat# 80204) and quantified using nanodrop. Reverse transcription was carried out using high capacity cDNA reverse transcription kit (Applied Biosystems, Warrington, UK cat # 4368814). Quantitative measurement of target gene expression relative to GAPDH was performed in triplicates using Power SYBR Green PCR Master Mix (Applied Biosystems, Warrington, UK cat # 4368706) following the manufacturer's recommendations in an ABI 7900HT Fast real Time PCR system. Relative expression was defined by  $2^{-\Delta Ct}$ , where  $\Delta Ct = Ct_{\text{target gene}} - Ct_{\text{GAPDH}}$ . The primer sequences are given in the [S2 Table](#).

### Tracking cell division by CFSE staining following vismodegib treatment

Single cell suspensions of neurospheres were stained with Carboxyfluorescein succinimidyl ester (CFSE) using CellTrace CFSE Cell Proliferation Kit (Life technologies, Oregon, USA cat# C34554) following manufacturer's protocol. The stained cells were divided into two equal parts, one part treated with DMSO and the other part was treated with 50 $\mu$ M vismodegib for 5 days. CFSE staining intensities were measured by flow cytometry (BD Acuri C6, BD Biosciences, USA) after 5 days of treatment.

### Annexin V staining for apoptosis

Approximately  $10^6$  cells/ml were seeded in 6-well plates and treated with either DMSO or 50 $\mu$ M vismodegib consecutively for 5 days. At the end of 5 days the cells were harvested and stained with annexin V. Annexin V staining was done using Alexa Fluor 488 Annexin V/Dead Cell Apoptosis Kit (Life technologies, Oregon, USA cat# V13241) following manufacturer's protocol.

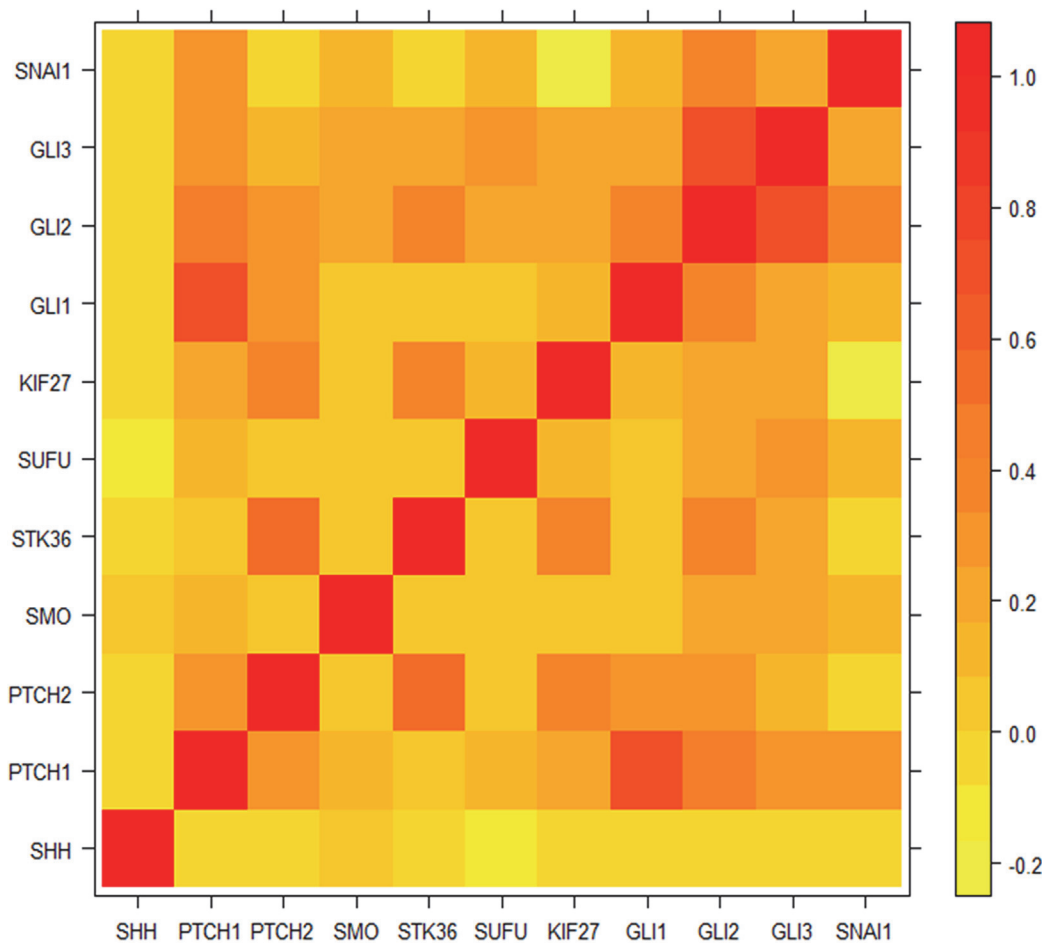
### Statistical analysis

Pearson's correlation coefficients ( $r$ ) were determined on the expression of 11 canonical Hh-pathway component genes in TCGA-GBM cases. Multiple testing correction (MTC) was done with a False Discovery Rate (FDR) of 0.1, to find out significant correlations (cut-off of statistical significance  $|r| > 0.17$ ). Student's t-test was used to compare GLI1 mRNA expressions between MB, GBM patients and patient-derived neurospheres. To compare the differences in apoptotic cell numbers (annexin V positive cells) of DMSO- and vismodegib-treated cells, for the  $i^{\text{th}}$  set of experiments, we translated the number of viable vismodegib-treated cells as percentage of viable DMSO-treated cells ( $u_i$ ). The mean of  $u_i$  was compared with 100, using univariate t-test. Dose-dependent changes of GLI1 expression in neurospheres were tested by ANOVA followed by multiple comparison tests. All statistical analyses were done using R (<http://www.r-project.org>) and GraphPad Prism 6 (<http://www.graphpad.com>).

## Results

### Expression correlations of canonical Hh-pathway component genes in GBM

A strong correlation ( $r = 0.7$ ) between *GLI1* and *PTCH1* mRNA expression was observed among the 149 cases of TCGA-GBM database as shown in Fig. 1. This is a hallmark of Hh-pathway activity [19]. Statistically significant correlations of mRNA expression of *GLI1* with that of the other two Hh-transcription factors, *GLI2* ( $r = 0.34$ ) and *GLI3* ( $r = 0.21$ ) were also observed. Other than this, significant correlations (correlations above significance cut-off  $|r| = 0.17$ ) between intermediate Hh-pathway component gene *STK36* with *PTCH2* ( $r = 0.58$ ), *KIF27* ( $r = 0.37$ ), *GLI2* ( $r = 0.34$ ) and *GLI3* ( $r = 0.21$ ) were observed. Hh-pathway downstream target *SNAI1* mRNA expression was significantly correlated with that of *PTCH1* ( $r = 0.29$ ), *GLI2* ( $r = 0.38$ ) and *GLI3* ( $r = 0.24$ ). Cumulatively these correlation patterns are suggestive of activity of the canonical Hh-pathway in this malignancy.



GBM TCGA (N=149)  
RNASeq V2 platform

**Fig 1. Heat map of correlation matrix for the expression of 11 canonical Hh-pathway component genes in TCGA-GBM (N = 149, significant cut-off  $|r| > 0.17$ , MTC with FDR 0.1).**

doi:10.1371/journal.pone.0116390.g001

### GLI1 mRNA expression pattern in GBM shows a single continuous distribution rather than discrete high- or low- GLI1-expressing clusters

In order to estimate the quantitative levels of GLI1 mRNA expression in GBM—how high is “high” and how low is “low”—we compared GLI1 mRNA expression of NIBMG-GBM clinical cohort (N = 19) with that of an already published clinical cohort of MB (N = 56) [19]. Along with these 56 cases we included a single MB case from our repository in the analysis. Log scale distribution of GLI1 mRNA expression ( $2^{-\Delta Ct}$  values) in MB showed two discrete clusters as high- and low- Hh MB groups as shown in Fig. 2A. The single case of MB from our NIBMG repository was clustered along with the other 12 high-Hh-MB patients. Unlike MB, no such discrete high- or low- Hh clusters in GBM was observed despite the differences between minimum and maximum levels of GLI1 mRNA expression within the same cohort of GBM varying within 3 orders of magnitude (Fig. 2B and C). Similarly, the minimum and maximum GLI1 mRNA expression among the GBM neurospheres also varied in 2 orders of magnitude (Fig. 2D). The median GLI1 mRNA expression of NIBMG-GBM (N = 19) when compared with that of the high-Hh-MB (N = 13) and with the low-Hh-MB (N = 44), it was found to be 14.8 fold lower (p-value 3.04604E-06) than that of the high-Hh-MB but 5.6 fold higher (p-value 0.00367) than that of the low-Hh-MB. There was no significant difference (p-value

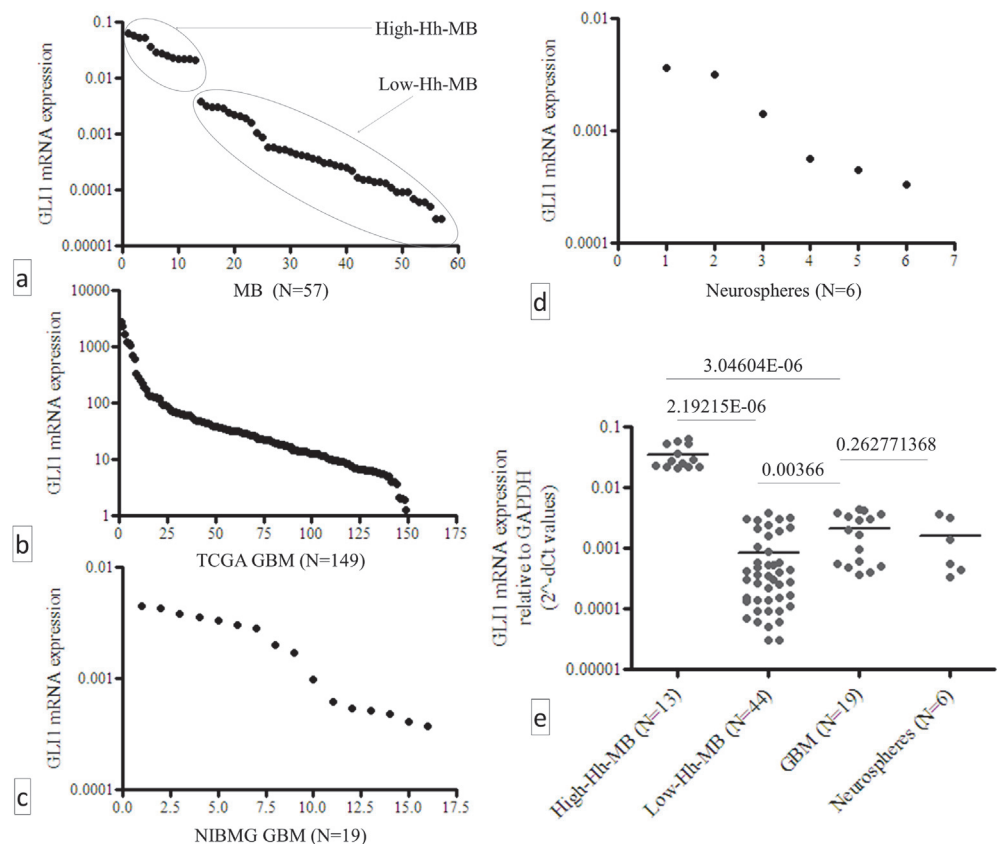


**Fig 2. Log scale distribution of GLI1 mRNA expression in a) already published MB cases, along with 1 new case of MB from our repository b) distribution of GLI1 mRNA expression (RNA-Seq data) of the TCGA-GBM sub-cohort (N = 149), c) distribution of GLI1 mRNA expression in NIBMG-GBM cases (N = 19), d) distribution of GLI1 mRNA expression in GBM patient-derived early passage neurospheres (N = 6) and e) comparison of median GLI1 mRNA expression levels of high-Hh-MB (N = 13), low-Hh-MB (N=44), NIBMG-GBM (N = 19) and GBM patient-derived neurospheres (N = 6).**

doi:10.1371/journal.pone.0116390.g002

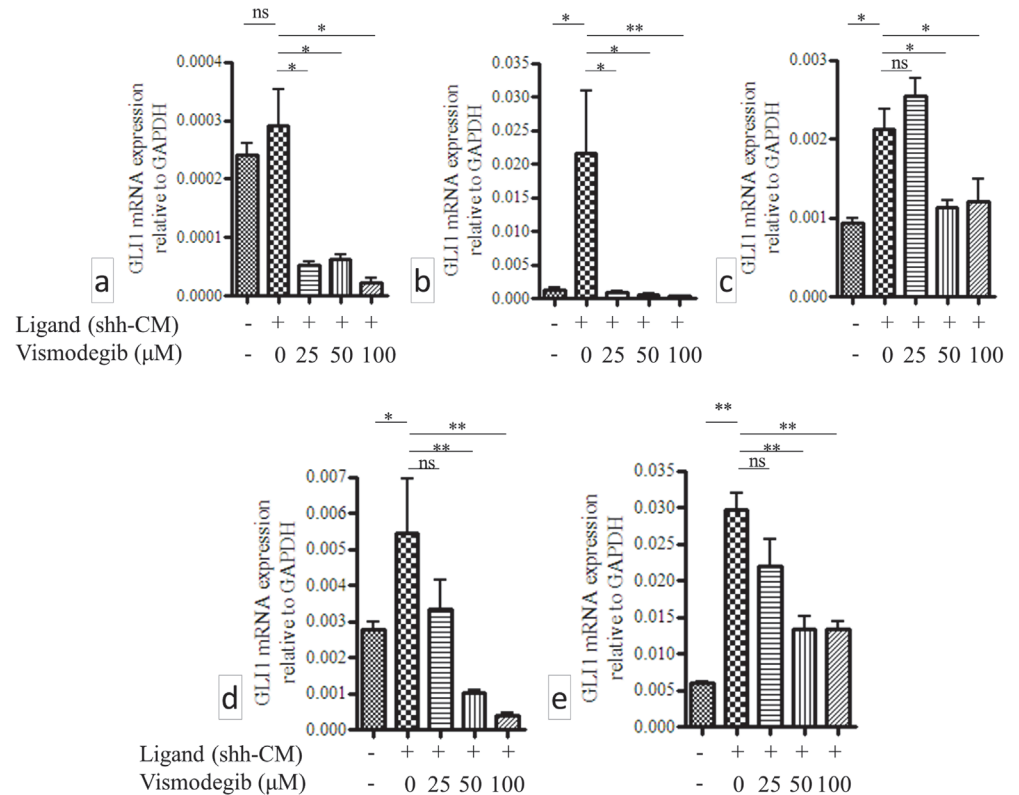


**Fig 3. Ligand driven up-regulation and vismodegib driven down-regulation of GLI1 mRNA expressions in 5 GBM neurospheres a) A49910, b) B0027, c) B0043, d) B0051 and e) M45481 (\* p-value < 0.05, \*\* p-value < 0.01, \*\*\* p-value 0.001 and ns, not significant).**

doi:10.1371/journal.pone.0116390.g003

0.2627) observed between the median GLI1 levels of NIBMG-GBM patients and patient-derived neurospheres, as shown in Fig. 2E.

### Ligand-driven up-regulation and vismodegib-driven down-regulation of GLI1 mRNA expression in GBM neurospheres *in vitro*

Next, we demonstrated direct up- and down- regulation of Hh-pathway activity in GBM neurospheres *in vitro* (N = 5) by Hh ligand (shh-CM) and clinically relevant doses of vismodegib (25μM, 50μM and 100μM) respectively. As shown in Fig. 3 there was statistically significant up-regulation of GLI1 mRNA expression in 4 out of 5 GBM neurospheres when treated with 50% (v/v) Shh-CM *in vitro*. Significant down-regulation of GLI1 mRNA levels in a dose-dependent manner was observed in all 5 neurospheres at 3 different clinically relevant doses of vismodegib (Fig. 3).

### Vismodegib induces apoptosis and cell cycle arrest in GBM neurospheres *in vitro*

Finally, we tested if clinically achievable dose (50μM) of vismodegib exerts an effect on cellular proliferation and apoptosis of GBM neurospheres *in vitro* irrespective of their relative endogenous levels of GLI1 mRNA expression. As shown in Fig. 4A B and C, neurospheres with relatively lower endogenous level of GLI1 mRNA expression (as shown in Fig. 3 B) and neurospheres with relatively higher endogenous level of GLI1 mRNA expression both showed

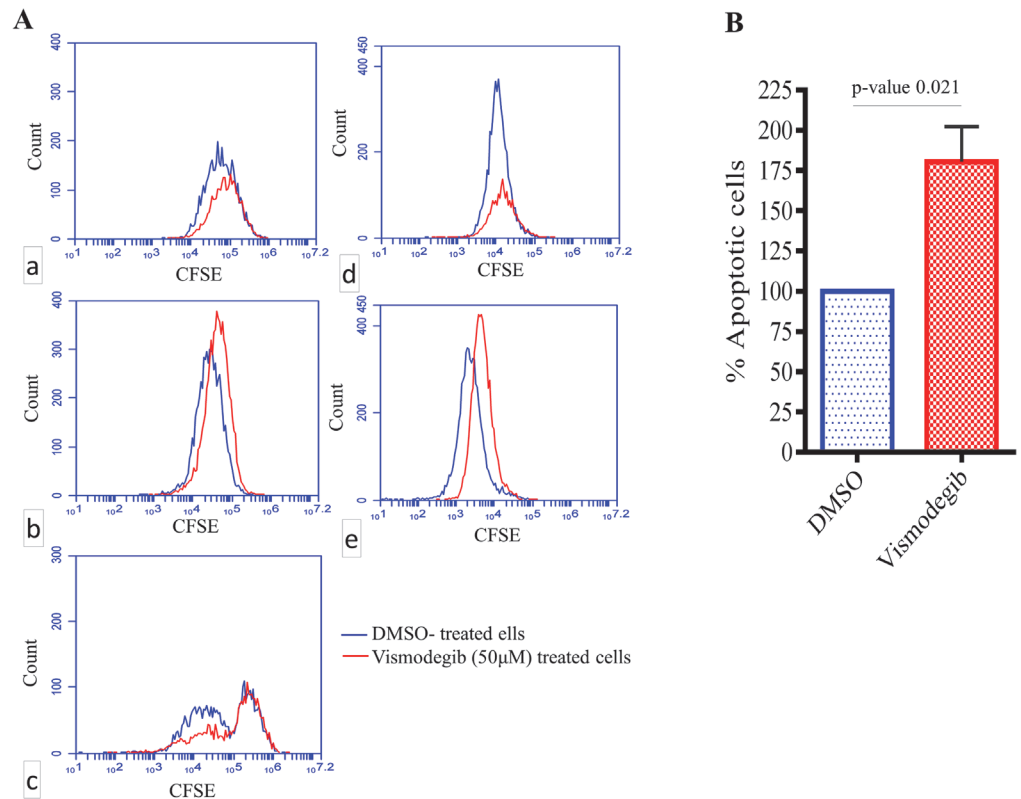


**Fig 4. A, cell cycle arrest in GBM neurospheres with vismodegib treatment *in vitro* a) A49910, b), B0027, c) B0043, d) B0051 and e) M45481. B, Number of apoptotic cells (annexin V positive) in GBM neurospheres treated either with DMSO or with 50  $\mu$ M vismodegib.**

doi:10.1371/journal.pone.0116390.g004

cell cycle arrest with vismodegib treatment, as demonstrated by CFSE staining. However, rest of the three neurospheres did not show any growth arrest but a 1.75 fold increase (p-value 0.021) in the average number of apoptotic cells in all of them (N = 5) was observed when treated with similar dose (50  $\mu$ M) of vismodegib for 5 days *in vitro*. Induction of apoptosis was demonstrated by annexin-V positive cells in vismodegib-treated neurospheres compared to their DMSO-treated controls (Fig. 4B). Altogether, the effect of ligand-driven up-regulation, vismodegib-driven down regulation of GLI1 mRNA expression levels (Fig. 3) and also induction of apoptosis/cell cycle arrest in the GBM patient-derived neurospheres (Fig. 4A and B) were observed irrespective of their relative endogenous levels of GLI1 mRNA expression.

## Discussion

In this paper we revisited the role of Hh-pathway in GBM upon the availability of TCGA-GBM database. First time we demonstrated here a strong expression correlation of GLI1 with PTCH1 expression by utilizing the large clinical cohort of TCGA-GBM database. Strong correlation of GLI1 and PTCH1 expression is a hallmark of Hh-pathway activity [19], since PTCH1 is a bona fide target of GLI1 transcription factor [11], confirming the relevance of this pathway in this malignancy. The previous disagreements on Hh-pathway activity in this malignancy, as presented in the introduction section of this manuscript [24], might have been because of including smaller sample sizes—since the inter- and intra- tumor heterogeneity in GBM could be notorious.

Although GLI1/PTCH1 correlation confirmed the relevance of Hh-pathway in GBM, we sought comparative quantitation of GLI1 mRNA expression in this malignancy—how low is

“low” and how high is “high”—compared to another lethal CNS malignancy such as MB [19]. We used MB as a reference because the role of Hh-pathway is more clearly known in this malignancy. Since we used the same set of qRT-PCR primers to estimate GLI1 expression in both MB and NIBMG-GBM, the  $2^{-\Delta C_t}$  values were comparable. GLI1 mRNA expression of the single MB case from our repository, which was included in the study, clustered along with the other 12 high-Hh-MB cases, substantiating consistency of our method of estimation. Interestingly, we observed median GLI1 mRNA expression in GBM to be significantly lower than that of the high-Hh-MB patients but significantly higher than that of the low-Hh-MB patients. A plausible explanation of this observation is as follows. Hh-pathway activity is driven by a loss-of-function mutation of PTCH1 gene—which is a negative feed-back regulator of Hh-pathway—in case of MB and in BCC [28]. Since the negative feedback regulator of the pathway (PTCH1) is mutated in MB the overall levels of the pathway activity, as estimated by GLI1 expression levels, is un-attenuated and remains higher compared to malignancies where PTCH1 is wild type. Malignancies where PTCH1 is wild type—such as in GBM, pancreatic cancer, ovarian cancers etc.—the resultant effect of ligand-driven aberrant activation of Hh-pathway might be “dampened” or “mellowed down” by PTCH1-mediated negative feed-back mechanisms. However, it is a subject to a far more detailed investigation comparing several malignancies across the board in order to generalize this concept of relative quantitation of Hh-pathway activity between malignancies—particularly between malignancies where the aberrant activity of this pathway is ligand-driven versus it is PTCH1 mutation-driven. Our analysis revealed, unlike MB, GLI1 mRNA expression in GBM to have a single continuous distribution rather than discrete high- or low- Hh expressing clusters. This distribution pattern needs to be taken into account while recruiting GBM patients in clinical trials for therapies with Hh-inhibitors. Technically there is no discrete “cut-off” for high-Hh or low-Hh expressing GBM in order to stratify patients for therapy with Hh inhibitor drugs, despite the inter-tumor differences in GLI1 expression among the patients varied in 3 orders of magnitude. Similar pattern was observed in GBM patient-derived neurospheres as well. Therefore, we sought to determine if there was a direct effect of Hh inhibition by vismodegib (GDC-0449), a pharmacological inhibitor of Hh-pathway and a clinically approved anticancer drug [18], on these GBM neurospheres *in vitro* irrespective of their relative endogenous levels of GLI1 mRNA expression. We clearly demonstrated statistically significant ligand-driven up-regulation of GLI1 mRNA expression and statistically significant vismodegib-driven down-regulation of GLI1 mRNA expression by 3 clinically relevant doses of vismodegib in a dose dependent manner in GBM neurospheres *in vitro*. Also, we demonstrated induction of apoptosis/cell cycle arrest in the GBM neoplastic cells *in vitro* with clinically achievable dose of vismodegib, irrespective of their relative endogenous levels of GLI1 mRNA expression. However, the induction of apoptosis by vismodegib treatment to the GBM neurospheres *in vitro* was statistically significant albeit the overall effect size was small, suggesting a further investigation in order to improve the effect of Hh-pathway inhibitor therapies in this malignancy. Our study is suggestive of this single continuous distribution pattern of GLI1 mRNA expression technically putting almost all GBM patients in a single group in terms of Hh-pathway activity. That is encouraging for therapies with Hh-pathway inhibitor drugs without a need for stratification on the basis of relative endogenous levels of Hh-pathway activity among tumors.

## Supporting Information

**S1 Table. Demography of the patients included in the study.** [S1 Table](#) contains list of the 19 GBM patients that were included in the study. (XLS)

**S2 Table. List of primers.** [S2 Table](#) contains sequences of primers that were used in quantitative RT-PCR experiments.  
(XLS)

## Acknowledgments

We thank all the patients and patient families for their kind cooperation and constant support. We thank Biswanath Bhattacharya, NIBMG, for helping with patient records and following up patients in clinic. We are especially thankful to Dr. Robert Yauch, Genentech, USA, for helping us with the medulloblastoma data. We acknowledge the members of NIBMG Bioinformatics laboratory for their kind help and cooperation. This work was supported by an intramural fund of NIBMG.

## Author Contributions

Conceived and designed the experiments: S. Dhara. Performed the experiments: VC TD PG SR UC SNG S. Deb SKS AKC SG S. Dhara. Analyzed the data: NKB AM AB S. Dhara. Contributed reagents/materials/analysis tools: PG SR UC SNG S. Deb SKS AKC SG CMR S. Dhara. Wrote the paper: S. Dhara.

## References

1. Nusslein-Volhard C, Wieschaus E (1980) Mutations affecting segment number and polarity in *Drosophila*. *Nature* 287: 795–801. PMID: [6776413](#)
2. Amakye D, Jagani Z, Dorsch M (2013) Unraveling the therapeutic potential of the Hedgehog pathway in cancer. *Nature medicine* 19: 1410–1422. doi: [10.1038/nm.3389](#) PMID: [24202394](#)
3. Ng JM, Curran T (2011) The Hedgehog's tale: developing strategies for targeting cancer. *Nature reviews* 11: 493–501. doi: [10.1038/nrc3079](#) PMID: [21614026](#)
4. Rubin LL, de Sauvage FJ (2006) Targeting the Hedgehog pathway in cancer. *Nat Rev Drug Discov* 5: 1026–1033. PMID: [17139287](#)
5. McMahon AP, Ingham PW, Tabin CJ (2003) Developmental roles and clinical significance of hedgehog signaling. *Current topics in developmental biology* 53: 1–114. PMID: [12509125](#)
6. Hahn H, Wicking C, Zaphiropoulos PG, Gailani MR, Shanley S, et al. (1996) Mutations of the human homolog of *Drosophila* patched in the nevoid basal cell carcinoma syndrome. *Cell* 85: 841–851. PMID: [8681379](#)
7. Gorlin RJ, Goltz RW (1960) Multiple nevoid basal-cell epithelioma, jaw cysts and bifid rib. A syndrome. *The New England journal of medicine* 262: 908–912. PMID: [13851319](#)
8. Gorlin RJ (1995) Nevoid basal cell carcinoma syndrome. *Dermatologic clinics* 13: 113–125. PMID: [7712637](#)
9. Rahnama F, Toftgard R, Zaphiropoulos PG (2004) Distinct roles of PTCH2 splice variants in Hedgehog signalling. *The Biochemical journal* 378: 325–334. PMID: [14613484](#)
10. Zaphiropoulos PG, Unden AB, Rahnama F, Hollingsworth RE, Toftgard R (1999) PTCH2, a novel human patched gene, undergoing alternative splicing and up-regulated in basal cell carcinomas. *Cancer research* 59: 787–792. PMID: [10029063](#)
11. Scales SJ, de Sauvage FJ (2009) Mechanisms of Hedgehog pathway activation in cancer and implications for therapy. *Trends in pharmacological sciences* 30: 303–312. doi: [10.1016/j.tips.2009.03.007](#) PMID: [19443052](#)
12. Li X, Deng W, Nail CD, Bailey SK, Kraus MH, et al. (2006) Snail induction is an early response to Gli1 that determines the efficiency of epithelial transformation. *Oncogene* 25: 609–621. PMID: [16158046](#)
13. Ruiz i Altaba A, Mas C, Stecca B (2007) The Gli code: an information nexus regulating cell fate, stemness and cancer. *Trends in cell biology* 17: 438–447. PMID: [17845852](#)
14. Gailani MR, Stahle-Backdahl M, Leffell DJ, Glynn M, Zaphiropoulos PG, et al. (1996) The role of the human homologue of *Drosophila* patched in sporadic basal cell carcinomas. *Nature genetics* 14: 78–81. PMID: [8782823](#)
15. Raffel C, Jenkins RB, Frederick L, Hebrink D, Alderete B, et al. (1997) Sporadic medulloblastomas contain PTCH mutations. *Cancer research* 57: 842–845. PMID: [9041183](#)



16. Yauch RL, Gould SE, Scales SJ, Tang T, Tian H, et al. (2008) A paracrine requirement for hedgehog signalling in cancer. *Nature* 455: 406–410. doi: [10.1038/nature07275](https://doi.org/10.1038/nature07275) PMID: [18754008](https://pubmed.ncbi.nlm.nih.gov/18754008/)
17. Low JA, de Sauvage FJ (2010) Clinical experience with Hedgehog pathway inhibitors. *J Clin Oncol* 28: 5321–5326. doi: [10.1200/JCO.2010.27.9943](https://doi.org/10.1200/JCO.2010.27.9943) PMID: [21041712](https://pubmed.ncbi.nlm.nih.gov/21041712/)
18. Rudin CM (2012) Vismodegib. *Clin Cancer Res* 18: 3218–3222. doi: [10.1158/1078-0432.CCR-12-0568](https://doi.org/10.1158/1078-0432.CCR-12-0568) PMID: [22679179](https://pubmed.ncbi.nlm.nih.gov/22679179/)
19. Rudin CM, Hann CL, Laterra J, Yauch RL, Callahan CA, et al. (2009) Treatment of medulloblastoma with hedgehog pathway inhibitor GDC-0449. *The New England journal of medicine* 361: 1173–1178. doi: [10.1056/NEJMoa0902903](https://doi.org/10.1056/NEJMoa0902903) PMID: [19726761](https://pubmed.ncbi.nlm.nih.gov/19726761/)
20. Berlin J, Bendell JC, Hart LL, Firdaus I, Gore I, et al. (2013) A randomized phase II trial of vismodegib versus placebo with FOLFOX or FOLFIRI and bevacizumab in patients with previously untreated metastatic colorectal cancer. *Clin Cancer Res* 19: 258–267. doi: [10.1158/1078-0432.CCR-12-1800](https://doi.org/10.1158/1078-0432.CCR-12-1800) PMID: [23082002](https://pubmed.ncbi.nlm.nih.gov/23082002/)
21. Kaye SB, Fehrenbacher L, Holloway R, Amit A, Karlan B, et al. (2012) A phase II, randomized, placebo-controlled study of vismodegib as maintenance therapy in patients with ovarian cancer in second or third complete remission. *Clin Cancer Res* 18: 6509–6518. doi: [10.1158/1078-0432.CCR-12-1796](https://doi.org/10.1158/1078-0432.CCR-12-1796) PMID: [23032746](https://pubmed.ncbi.nlm.nih.gov/23032746/)
22. Stupp R, Mason WP, van den Bent MJ, Weller M, Fisher B, et al. (2005) Radiotherapy plus concomitant and adjuvant temozolomide for glioblastoma. *The New England journal of medicine* 352: 987–996. PMID: [15758009](https://pubmed.ncbi.nlm.nih.gov/15758009/)
23. Dahmane N, Sanchez P, Gitton Y, Palma V, Sun T, et al. (2001) The Sonic Hedgehog-Gli pathway regulates dorsal brain growth and tumorigenesis. *Development (Cambridge, England)* 128: 5201–5212. PMID: [11748155](https://pubmed.ncbi.nlm.nih.gov/11748155/)
24. Hu Z, Bonifas JM, Aragon G, Kopelovich L, Liang Y, et al. (2003) Evidence for lack of enhanced hedgehog target gene expression in common extracutaneous tumors. *Cancer research* 63: 923–928. PMID: [12615704](https://pubmed.ncbi.nlm.nih.gov/12615704/)
25. Bar EE, Chaudhry A, Lin A, Fan X, Schreck K, et al. (2007) Cyclopamine-mediated hedgehog pathway inhibition depletes stem-like cancer cells in glioblastoma. *Stem cells (Dayton, Ohio)* 25: 2524–2533. PMID: [17628016](https://pubmed.ncbi.nlm.nih.gov/17628016/)
26. Gruber Filbin M, Dabral SK, Pazyra-Murphy MF, Ramkissoon S, Kung AL, et al. (2013) Coordinate activation of Shh and PI3K signaling in PTEN-deficient glioblastoma: new therapeutic opportunities. *Nature medicine* 19: 1518–1523. doi: [10.1038/nm.3328](https://doi.org/10.1038/nm.3328) PMID: [24076665](https://pubmed.ncbi.nlm.nih.gov/24076665/)
27. Brennan CW, Verhaak RG, McKenna A, Campos B, Nounshmehr H, et al. (2013) The somatic genomic landscape of glioblastoma. *Cell* 155: 462–477. doi: [10.1016/j.cell.2013.09.034](https://doi.org/10.1016/j.cell.2013.09.034) PMID: [24120142](https://pubmed.ncbi.nlm.nih.gov/24120142/)
28. Johnson RL, Rothman AL, Xie J, Goodrich LV, Bare JW, et al. (1996) Human homolog of patched, a candidate gene for the basal cell nevus syndrome. *Science (New York, NY)* 272: 1668–1671. PMID: [8658145](https://pubmed.ncbi.nlm.nih.gov/8658145/)